Geologica Acta, Vol.8, Nº 4, December 2010, 349-371
DOI: 10.1344/105.000001577
Available online at www.geologica-acta.com

geologica acta

Did Patagonia collide with Gondwana in the Late Paleozoic? Some insights from a multidisciplinary study of magmatic units of the North Patagonian Massif

A.E. RAPALINI [1] **M. LÓPEZ DE LUCHI** [2] **C. MARTÍNEZ DOPICO** [1] **F. LINCE KLINGER** [3] **M. GIMÉNEZ** [3] **P. MARTÍNEZ** [3]

[1] **Instituto de Geofísica Daniel A.Valencio, Departamento de Ciencias Geológicas, FCEyN, Universidad de Buenos Aires, CONICET**
Pabellón 2, Ciudad Universitaria, Buenos Aires, Argentina. Rapalini E-mail: rapalini@gl.fcen.uba.ar

[2] **Instituto de Geocronología y Geología Isotópica (INGEIS), Universidad de Buenos Aires-CONICET**

[3] **Instituto Sismológico Volponi, Universidad Nacional de San Juan, CONICET**

ABSTRACT

The origin of Patagonia and its relations with the South American crustal blocks to the north have been a matter of debate for decades. We report results from a multidisciplinary study centered on Paleozoic granitoids exposed in the northeastern corner of the North Patagonian Massif. Microstructural and magnetofabric studies reveal two suites of granitoids. Late Carboniferous (?) granitoids (Yaminué Complex, Tardugno Granodiorite, Cabeza de Vaca leucogranite) were emplaced and subsequently deformed in a major NNE-SSW compressive stress regime that also provoked top-to-the-SW thrust deformation in shallow crustal levels. Gravity and geobarometric studies show that the same major deformation event has been recorded at different crustal levels. The age and type of deformation of this event recorded across the northern boundary of Patagonia strongly supports a Late Carboniferous – Early Permian frontal collision between Patagonia and Gondwana. This major deformation event ceased by 281 Ma when the Navarrete Plutonic Complex, which shows mainly magmatic fabrics, was emplaced under a far-field WNW-ESE stress regime. Crustal continuity between the North Patagonian Massif and the Pampia and Arequipa-Antofalla terranes is suggested by similar Late Paleoproterozoic crustal model ages, comparable detrital zircon ages in Early Paleozoic successions, the apparent continuity of an Early Ordovician continental magmatic arc and paleomagnetic data. Reconciliation of this evidence with the Late Paleozoic frontal collision is obtained in a tectonic model that suggests that the North Patagonian Massif is a parautochthonous crustal block.

KEYWORDS | **Patagonia. Gondwana. Late Paleozoic. Collision. Magmatism.**

INTRODUCTION

The geologic evolution of Patagonia in pre-Mesozoic times is still a matter of debate. Two main hypothesis have been put forward. One suggests that Patagonia has always been an integral part of Gondwana (e.g. Dalla Salda et al., 1990) while an opposite view has portrayed Patagonia as an allochthonous terrane that collided with Gondwana in

Late Paleozoic times (e.g. Ramos, 1984, 2008). Numerous evidence in favor of one or another model has been produced and published in the last decade (e.g. Tickyj et al., 1997; Rapalini, 1998, 2005; Gonzalez et al., 2002; von Gosen, 2003; Chernicoff and Zappettini, 2003; Kostadinoff et al., 2005; Pankhurst et al., 2006; Gregori et al., 2008; and many others).

The basement of Patagonia has been traditionally subdivided into two tectonic blocks, i.e the North Patagonian or Somuncura Massif (NPM)- in the north- and the Deseado Massif in the south (Leanza, 1958, Harrington, 1962) (Fig.1). The relations among these blocks are poorly known (Ramos, 2002, 2008), as their mutual boundary is covered by thick Mesozoic to Cenozoic sedimentary successions of the San Jorge Basin (Uliana and Biddle, 1987). Recently, Pankhurst et al. (2006) suggested that while the NPM was already part of Gondwana in Ordovician times, southern Patagonia (basically the Deseado Massif) constitutes an allochthonous terrane that collided with the NPM in Mid-Carboniferous times. Ramos (2008, and references therein) also suggested a Paleozoic collision between the Deseado Massif and NPM. However, in his model southwestern Patagonia plus the Antarctic Peninsula ("Antonia" terrane), collided first with the NPM and then both collided with Gondwana in the Late Paleozoic. Paleomagnetic data obtained so far from the NPM suggest that this block shares a common apparent polar wander path with Gondwana since the Devonian (Rapalini, 1998). This is consistent with models that favor an autochthonous NPM, although the data still allow orthogonal movements between both land masses of the order of 1500 km (Rapalini, 2005). Pankhurst et al. (2006) provided strong geochronological evidence that the Early Ordovician magmatic arc that developed along the southwestern Gondwana margin (Famatinian arc, e.g. Pankhurst and Rapela, 1998 and references therein) extends into the NPM (Fig. 1a), which suggests crustal continuity between Gondwana and northern Patagonia in the Ordovician. From a detailed structural study on Early Paleozoic metasedimentary and clastic sedimentary rocks exposed in the northeastern NPM, von Gosen (2002, 2003) has documented an important NNE-SSW Late Paleozoic contractional event (Fig.1b) affecting this area, which would favor the model of a frontal collision between the NPM and Gondwana. Rapalini (2005) tried to reconcile both lines of evidence and suggested the possibility of a parautochthonous NPM that rifted away from Gondwana in the Early Paleozoic with the opening of a small ocean basin (≤ 1500 km) and its subsequent closure and collision in the Late Paleozoic. More recently, Gregori et al. (2008) acknowledged the important Late Paleozoic tectonic deformation along the northern boundary of

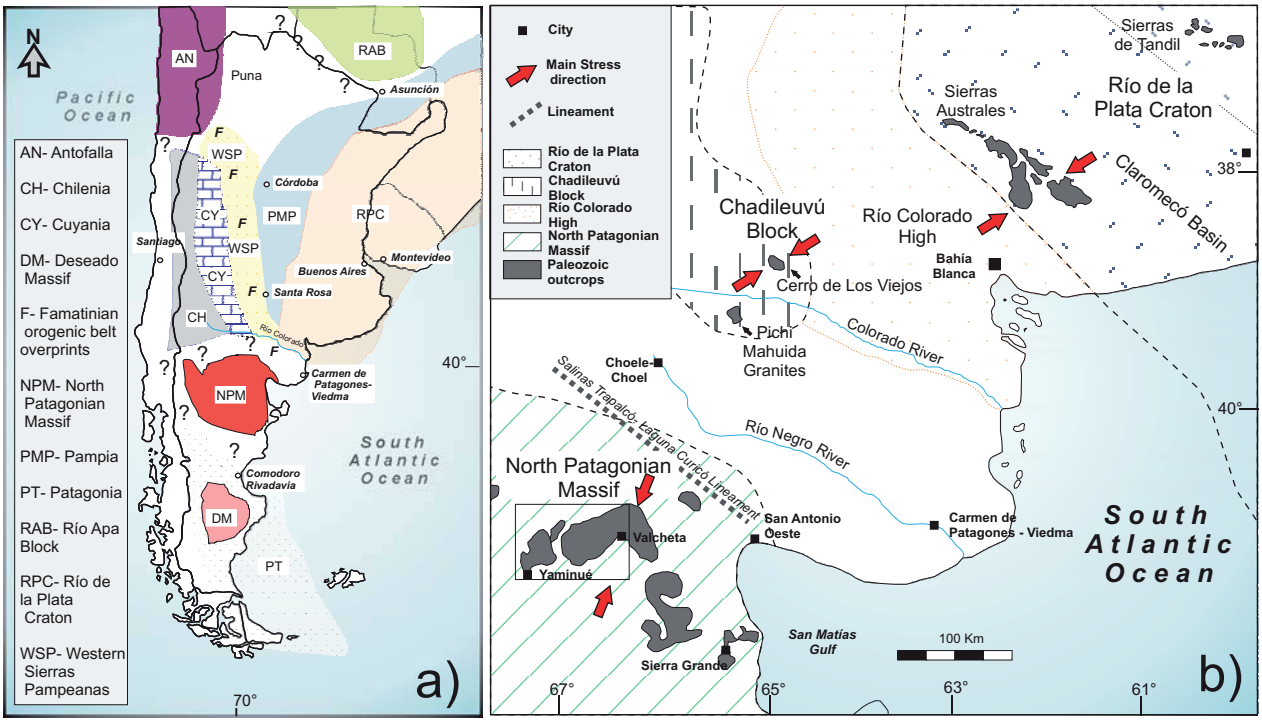

FIGURE 1 | **A) Schematic distribution of the major crustal units of the margin of West Gondwana, (modified after Rapalini, 2005 and Vaughan and Pankhurst, 2008 and references therein) using further information from Tohver et al. (2007) for the extension of the southern margin of the Río de la Plata craton; B) Geological sketch of the main tectonic elements between Sierras Australes and the northeastern North Patagonian Massif (modified after von Gosen, 2002; Gregori et al., 2008; Ramos, 2008). Rectangle corresponds to the geologic map of Figure 2.**

Patagonia and assigned it to a complex configuration of kinematically partially independent blocks, integrating the whole process into some kind of "escape tectonics". Different geophysical evidence has been used either to discard or to support crustal continuity between Gondwana and Patagonia. Chernicoff and Zappettini (2003) have interpreted regional aeromagnetic anomalies as suggesting a major crustal discontinuity along the northern boundary of the NPM whereas Kostadinoff et al. (2005) have proposed crustal continuity from regional gravity and magnetic information.

Late Paleozoic granitoids are relatively well exposed in northern Patagonia. They are interpreted in different ways according to the diverse tectonic models (Rapela and Caminos, 1987; Caminos, 2001; Llambías et al., 2002; Pankhurst et al., 2006; López de Luchi et al., 2010 and references therein). The relationship between magmatism and tectonic activity in the Late Paleozoic, the crucial time span for determining whether or not North Patagonia ever collided with the SW Gondwana margin, is discussed in this contribution. We integrate the results of a multidisciplinary study of the Late Paleozoic granitoids cropping out in the northeastern sector of the NPM, west of Valcheta. Detailed petrographic, isotopic and microstructural data were complemented with magnetic fabric studies, thermobarometric determinations and gravity surveys. In addition, new and published chronological information based on the Sm-Nd system was compiled and recalculated in order to characterize the crustal segment and processes involved in the petrogenesis of the granitoids in the northeastern part of the NPM. We put forward a tectonic model that favors the idea of a frontal collision between a paraautochthonous NPM and the Gondwana margin in the Late Carboniferous-Early Permian.

GEOLOGIC BACKGROUND

Late Paleozoic magmatism is widespread in northern Patagonia defining an approximately E-W magmatic belt of Late Carboniferous to Permian granitoids (see Ramos, 2008, and references therein). Our study was carried out in the northeastern area of the NPM (Fig.2), along this major magmatic belt. The oldest stratigraphic unit of the area (see Table 1) is the metaclastic Nahuel Niyeu Formation (NNF, Chernicoff and Caminos, 1996a) which comprises a thick sequence of meta-greywackes, siltstones, shales, local hornfels and scarce metavolcanics. Deposition of the NNF occurred after 515 Ma, according to U-Pb dating of detrital zircons (Pankhurst et al., 2006). As Ordovician leucogranitoids (Caminos et al., 2001; López de Luchi et al., 2008; Tohver et al., 2008; Gozálvez, 2009) intrude the metaclastic unit, deposition of NNF is bracketed between the Middle Cambrian and the Furongian. Chernicoff and Caminos (1996a) described three deformational events affecting the NNF. D2, the main phase of deformation, produced SW verging folds with a NW-SE trending axis that plunges 30º to the SE. D3 records a change from a NE-SW towards an E-W stress field. This is basically consistent with the structural observations of von Gosen (2003), who described significant evidence of a main deformational phase with top-to-SSW thrust tectonics affecting the NNF and the Siluro-Devonian Sierra Grande Formation. This thrusting event can therefore be dated as post-Devonian.

Ordovician muscovite-bearing leucogranites intrude the NNF close to Valcheta town (Figs 2 and 3). These granitoids outcrop as NNE elongated bodies. The presence of Ordovician granites in the area was proposed by Caminos (2001) based on lithologic comparisons with the Punta Sierra Formation (U-Pb SHRIMP ca. 475 Ma, Pankhurst et al., 2006) that crops out 200 km ESE (Fig. 2) from our study area, along the Atlantic coast, and which intrudes the El Jagüelito Formation. Recent K-Ar and Ar-Ar muscovite cooling ages for the leucogranites which intrude the NNF (López de Luchi et al., 2008; Tohver et al., 2008; Gozálvez, 2009) provided the first geochronologic evidence for significant Ordovician magmatism in our study area (Fig. 2). These results argue for a wider regional extent of the Ordovician magmatism in the NE corner of the NPM (López de Luchi et al., 2008), as previously proposed by Pankhurst et al. (2006).

The Silurian-Devonian marine sedimentary rocks of the Sierra Grande Formation (SGF) unconformably overlie the NNF. The SGF comprises quartzites, orthoquartzites and minor conglomerates and pelites. A Silurian to Early Devonian age has been assigned on the basis of scarce invertebrates (Manceñido and Damborenea, 1984). Recent dating of detrital zircons by U-Pb (SHRIMP) by Uriz et al. (2008a, b) indicates a maximum depositional age of 428 Ma. Outcrops of the SGF have been affected by Late Paleozoic folding and thrusting, both in its type-area near the town of Sierra Grande (Zanettini, 1981; von Gosen, 2002) as well as in our study region (von Gosen, 2003).

The Yaminué Complex (YC), originally defined by Caminos and Llambías (1984) and further studied by Chernicoff and Caminos (1996b), Llambías et al. (2002) and López de Luchi et al. (2010), comprises strongly foliated granitoids, emplaced in gneisses, schists and marbles of unknown age. The largest and best outcrops of this unit are located to the south of the Falkner and Ramos Mexia railway stations (Fig. 2). There, the YC (Fig. 3) forms NE shallowly dipping sheet-like bodies of a coarse to medium grained porphyritic granodiorite-monzogranite, and less frequently tonalite (López de Luchi et al., 2010). These are separated by sub-concordant sheets of mostly tonalitic biotite-orthogneiss, a fine-grained equigranular to porphy-

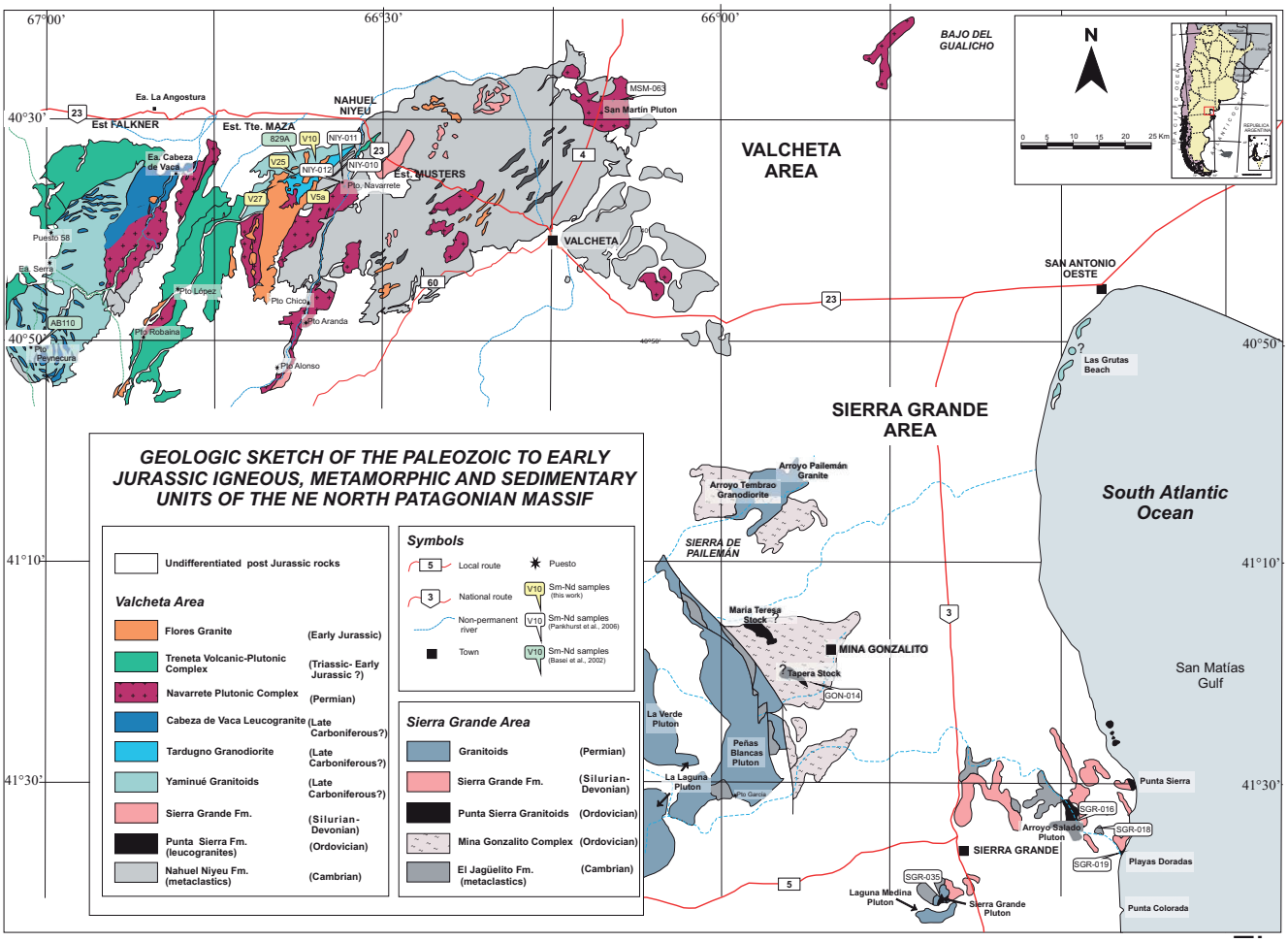

FIGURE 2 | **Geological sketch of the Paleozoic to early Jurassic units of Sierra Grande and Valcheta areas with the location of the sampling localities for Sm-Nd data.**

ritic leucogranite and some pegmatite dykes. At the central part of the complex, unfoliated tonalite and granodiorites with microgranular enclaves appear as isolated outcrops. The coarse porphyritic granodiorite-monzogranite dominates the middle part of the complex whereas the tonalite forms most of its base towards the south (López de Luchi et al., 2010). The YC shows both intrusive and tectonic contacts with the NNF at different localities (von Gosen, 2003). Chernicoff and Caminos (1996b) proposed that it was affected by two episodes of deformation. For many years this unit was considered as Precambrian (Caminos et al., 1994). More recently, Basei et al. (2002) suggested a Late Carboniferous age based on conventional U-Pb zircon dating. However, the ages are not very precise. Foliated granitoids with high temperature solid state deformation microstructures yielded ages at 305±31, 281± 29 and 276±11 Ma. An age of 244±14 Ma for a granitoid with a green-schist facies deformation overprint suggests episodes of lead loss.

The Tardugno Granodiorite (TG, Figs. 2 and 3) is exposed to the south of the Nahuel Niyeu village. It consists of deformed porphyritic granodiorites variably affected by a heterogeneously developed foliation that led to S-C surfaces (Chernicoff and Caminos, 1996b). Kinematic indicators demonstrate a top-to-the-SW sense of shear (von Gosen, 2003). This granodiorite is intruded by a tonalite of the Permian Navarrete Plutonic Complex and is in contact with the NNF along steeply dipping NE trending mylonitic shear zones. Basei et al. (2002) have reported a 300±6 Ma conventional U-Pb age for an undeformed tonalite assigned to the TG.

The recently defined Cabeza de Vaca Leucogranite (CVL, López de Luchi et al., 2010), corresponds to a large igneous body that intrudes the YC in the western sector of the study area near the Estancia Cabeza de Vaca (Fig. 3). This unit was previously considered as part of the Navarrete Plutonic Complex (Rapela and Caminos, 1987). Leucogranitic sheets and dykes intruding the granodiorite-tonalites of the YC over most of the western sector are also considered as part of this unit. The leucogranite sheets are concordant with the penetrative fabric of the tonalite-grano-

TABLE 1 | **Schematic stratigraphy, lithology, structural features and ages for the main pre-Cretaceous units of the Valcheta area, based on the works of Caminos (1983, 2001), Chernicoff and Caminos (1996a, b), Llambías et al. (2002), Basei et al. (2002), von Gosen (2003), Pankhurst et al. (2006), Uriz et al. (2008a), Tohver et al. (2008) and López de Luchi et al. (2008).**

Geologic Unit	Lithology	Structure and metamorphism	Age
Flores Granite	Bt leucogranite	Undeformed	193±5, 188±2 Ma (K-Ar, Msc), 188±3 Ma (Rb-Sr isochron)
Treneta Volcanics	Dacitic to rhyolitic efusives and dykes	Subhorizontal. Undeformed	Triassic (?)
Navarrete Plutonic Complex	Biotite-amphibole/amphibole biotite tonalite-garnodiorite Biotite monzogranite Monzodiorite	Undeformed. Far-field tectonic control in intrusion and emplacement mechanisms. Localized low temperature shear bands	281±3 Ma (U-Pb, SHRIMP, zircons) for the Aranda facies
Cabeza de Vaca Leucogranite	Biotite Leucogranite	Foliated	Latest Carboniferous (?)
Tardugno Granodiorite	Biotite Granodiorite-monzogranite	Foliated-, S-C surfaces	300±6 Ma (U-Pb conventional, zircons)
Yaminué Complex	Strongly foliated biotite granitoids, biotite orthogneisses,minor biotite-amphibole granodiorite	Stacked sheets of foliated granitoids, syn-emplacement to high and low temperature deformation. Low angle tectonic foliations and lineations	Late Carboniferous (?) (305±31, 281± 29 and 276±11 Ma, U-Pb conventional)
Sierra Grande Fm.	Quartzites, sandstones, conglomerates	No metamorphism. Folded and thrust faulted, mainly top to SSW thrusts	Silurian to Devonian. < 428 Ma (U-Pb SHRIMP, detrital zircons)
Punta Sierra Fm.	Muscovite leucogranite	Undeformed	Middle-Late Ordovician, 449±7 Ma (K-Ar. Msc), 454±2 Ma (Ar-Ar, Msc), 468±5 Ma (Ar-Ar, Msc)
Nahuel Niyeu Fm.	Schists, metasandstones, marbles, metavolcanics	Very low to low metamorphic degree. At least two deformational phases. Affected by top to SSW thrusts	Cambrian to Early Ordovician (?) < 515 Ma (U-Pb SHRIMP, detrital zircons)

diorite. These sheets were deformed into tight folds with NW- to NNW trending axes (Chernicoff and Caminos, 1996b). The inequigranular to equigranular fine-grained leucogranite consists of quartz, plagioclase (often saussuritised) and K-feldspar, with <5% biotite. At diffe-rent outcrops it appears either massive or well foliated. No radiometric dating is available for this unit, although intrusive relations and deformational history (López de Luchi et al., 2010) suggest an age bracketed between the YC and the Navarrete Plutonic complex.

The Navarrete Plutonic Complex (NPC) is the most conspicuous Late Paleozoic granitoid unit in the study area (Figs. 2 and 3). It is composed of granodiorites, tonalites, granites and associated microtonalite, microgranodiorite, microdiorite, spessartitic lamprophyres and leucogranitic dykes, which on the basis of major and some trace-elements were suggested to be related to a subduction zone magmatism (Rapela and Caminos, 1987). The largest outcrops (Fig. 3) are located to the south of the Nahuel Niyeu village (eastern outcrops, ca. 70 km^2) and the Falkner railway station (western outcrops, ca. 180 km^2). Scattered granitoid outcrops (Figs. 2 and 3), located to the west and north of Valcheta town, i.e. San Martín pluton, have also been assigned to the NPC (Caminos, 2001). Different facies have been identified in this complex (Rapela and Caminos, 1987; Caminos, 2001). López de Luchi et al. (2010) recently proposed the existence of three main facies: i) the Robaina Facies: a porphyritic biotite (±amphibole) granodiorite-monzogranite; ii) the Aranda Facies: a biotite-hornblende granodiorite; and iii) the Guanacos Facies: a porphyritic to equigranular amphibole-biotite tonalite-granodiorite.

In several areas the NPC is cut by early Jurassic epizonal granites (Flores granite) or covered by Triassic or younger volcanic rocks as well as modern sediments. Therefore, the actual shape of the plutonic bodies is difficult to determine from the exposures alone, with the exception of the eastern outcrops west of the Salado creek (Fig. 3). Contacts with the host rocks (generally the NNF metasediments) are discordant, sharp and strait. Only in a few places (e.g. Puesto Navarrete) the pluton borders are mostly concordant with the foliation of the surrounding metasedimentary rocks. On the western border of the western outcrops, where the NPC is intruding the YC, contacts are sharp at the meter scale (Caminos, 2001), but more irregular and transitional at a smaller scale. A SHRIMP zircon age of 281±3 Ma was obtained by Pankhurst et al. (2006) from a biotite granodiorite at Puesto Navarrete (Aranda facies, Fig. 2) suggesting an Early Permian age for the entire NPC. A lower quality U-Pb SHRIMP zircon crystallization age of ca. 260 Ma (Pankhurst et al., 2006) was reported for the San Martín pluton, exposed to the north of Valcheta (Figs. 2 and 3). Recently, López de Luchi et al. (2008) have provided a K-Ar age of 258±4 Ma on biotite from the San Martin pluton, consistent with the U-Pb age.

An erosional unconformity separates the NPC from the Treneta volcanics which are represented by Triassic (?) andesites, rhyolitic tuffs and dacitic ignimbrites. The early Jurassic Flores Granite (Rb/Sr isochron age of 188± 3 Ma, Pankhurst et al., 1993, and K-Ar cooling ages on muscovite of 188±2 and 193±5, Ma, López de Luchi et al., 2008) intrudes the NPC at the eastern outcrops mainly (Figs. 2 and 3).

STRUCTURAL DATA: MAGNETIC FABRICS AND MICROSTRUCTURES

Field and microscopic observations

López de Luchi et al. (2010) reported a detailed microstructural and magnetic fabric study of the Late Paleozoic

granitoids of the area west of Valcheta (Fig. 3). The studied units comprise the YC, the TG, the CVL and all facies of the NPC. Microscopic analyses of mineralogy, textures and microstructures permitted to characterize each unit. A brief summary of them follows:

The Late Carboniferous YC (Figs. 2 and 3) is dominated by foliated granitoids that exhibit either magmatic or solid-state deformation which developed a penetrative planar fabric and parallel high-strain zones, including meter- to decameter-sized sheets of orthogneisses, which are mostly tonalites. Magmatic microstructures are indicated by shape-preferred orientation of undeformed feldspar and biotite. Submagmatic microstructures (Bouchez et al., 1992) which correspond to melt relocation textures are observed as microaplite surrounding or filling fractures in perthitic K-feldspar crystals and in strain shadows or in shear bands around the feldspars. In the moderately solid-state deformed granitoids, foliation and lineation are defined by the preferred orientation of feldspars and micas. Megacrysts of K-feldspar, partially converted into microcline, show tails of recrystallized melt relocation aggregates. Quartz appears as flattened polycrystalline aggregates due to subgrain rotation and grain boundary migration recrystallization and shows relics of chess-board subgrains.

The TG is characterized by a dominant S-C fabric in which K-feldspar porphyroclasts locally show coarse core and mantle structures and contain flame perthites. Narrow shear zones with intense grain-size reduction zones cut the core-and-mantle fabrics of the feldspar. In more intensely deformed areas, the porphyroclasts form well-developed triple points. Biotite, chlorite and dynamically recrystallised quartz define the C surface. Kinked and bent muscovite occurs locally. Large quartz grains show elongate subgrains and contain dynamically recrystallised bands. Heterogeneously developed low temperature shear zones are observed near the contact with the NNF. The mylonites and ultramylonites developed in the TG have a pronounced NE trending steep planar fabric.

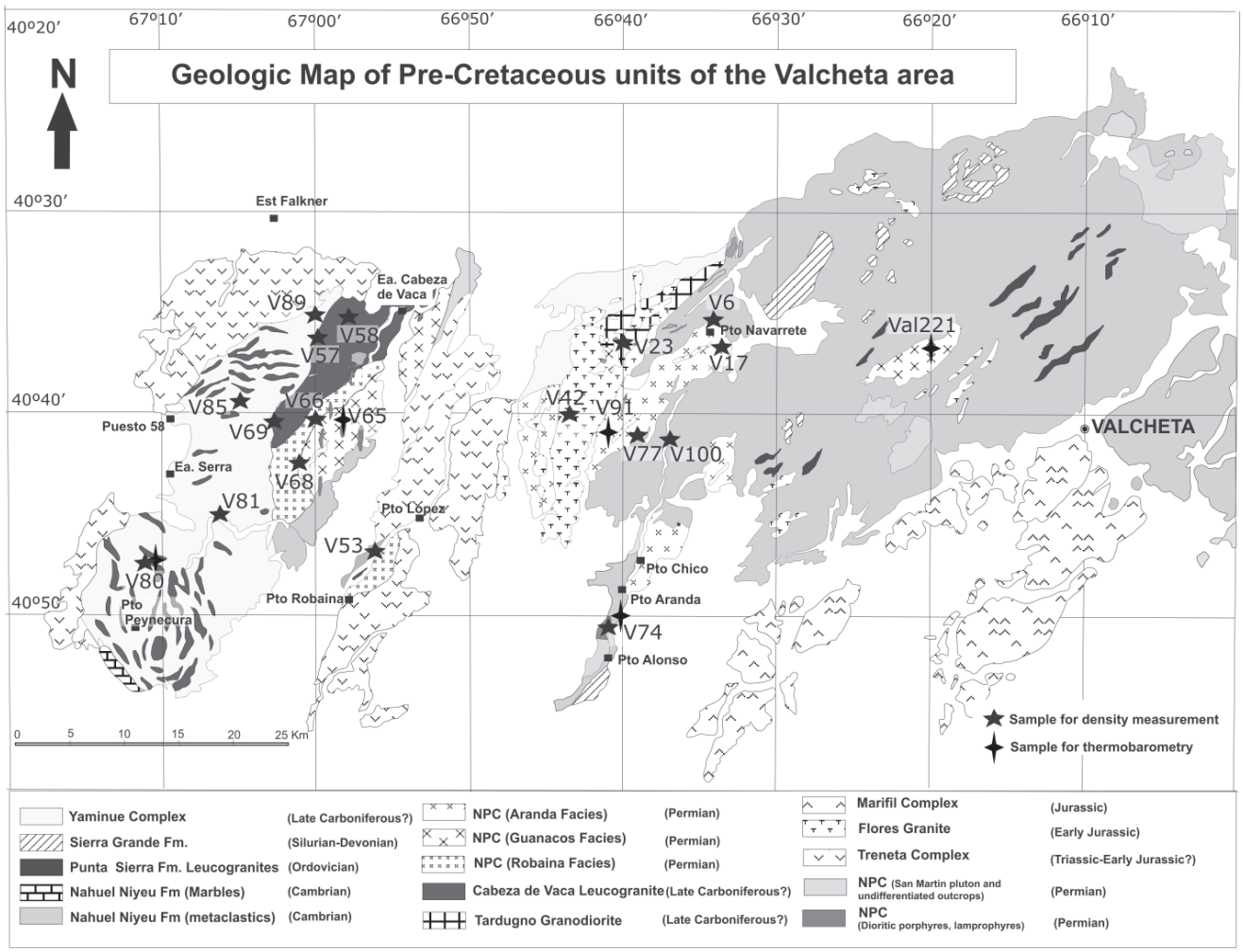

FIGURE 3 | **Geologic map of pre-Cretaceous units exposed west of Valcheta (from Caminos, 1983, 2001 and our own observations).**

The CVL appears either massive or well foliated. The variably developed solid-state foliation is defined by recrystallized flattened quartz aggregates which wrap around the K-feldspar porphyroclasts with evidence of both subgrain rotation and grain boundary migration recrystallization. In some samples melt relocation textures and submagmatic fractures would suggest a continuity of the deformation from the latest stages of crystallization to the initial stages of cooling.

The NPC is dominated by magmatic and submagmatic microstructures. The Robaina Facies is variably foliated due to a macroscopic, shape-preferred orientation of euhedral K-feldspar and biotite. Quartz crystals are subhedral with some undulose extinction and chessboard patterns but they are equant except in the more foliated types. Although high-temperature solid-state microstructures are identified towards the western border close to the western outcrops of the YC the overall magmatic texture remains unmodified. The Aranda Facies shows dominant coarse grained and equigranular to slightly porphyritic textures. K-feldspar varies from microcline to smoothly twinned perthitic orthoclase. Quartz is subhedral to anhedral and appears as monocrystalline or in aggregates. Deformation at the magmatic stage is shown by locally chessboard subgrains in quartz. In some cases a weak planar fabric is defined by the shape preferred orientation of subhedral plagioclase, biotite and some amphibole. Submagmatic deformation is evidenced by fractures in feldspar filled with microaplite, and some subgrains in plagioclase. The Guanacos Facies is characterized by coarse-grained grey hornblende-biotite tonalites predominantly homogeneous and massive that grade into granodiorite compositions. Although chessboard subgrains are observed in quartz the angular shape of the interstitial spaces is preserved. Anhedral to subhedral amphibole crystals appear as isolated crystals or tend to form clots. Submagmatic fractures filled with quartz and recrystallized fine-grained plagioclase mosaics are found towards the western margin of the facies.

The dominant facies of the San Martín Pluton is a pinkish porphyritic monzogranite with up to 4 cm K-feldspar megacrysts. Crystals of quartz and feldspar are surrounded by a fine-grained quartz–feldspar matrix, and undeformed biotite grains. Sometimes, small grains are included into larger grains and can form an inner corona near grain boundaries. This microstructure is interpreted as a melt relocation texture in which the fined-grained fraction is a result of late-magmatic melt crystallization.

Anisotropy of magnetic susceptibility (AMS)

These observations were complemented through the study of the magnetic fabric of the exposed granitoids (López de Luchi et al., 2010) by means of the anisotropy of magnetic susceptibility (AMS, Tarling and Hrouda, 1993). The experimental procedures and detailed interpretations were presented in López de Luchi et al. (2010). The most significant AMS results are presented in Figure 4 (see also Table I, available in the electronic version of the paper at www.geologica-acta.com). Sixty sampling sites (over 300 independent cores) were located on the outcrops of the above described units. While the NPC is basically ferromagnetic (mean bulk susceptibility $K > 10^{-3}$ SI), the CVL and TG plutons are paramagnetic ($K < 10^{-4}$ SI). On the other hand, the YC shows a large dispersion in bulk susceptibility values, consistent with its largest lithologic variation. In general, a good agreement between AMS scalar parameters as anisotropy degree (P', Jelinek, 1978) and deformation as observed microscopically was found. Shape parameter (T, Jelinek, 1978) showed a clear correlation between anisotropy degree and oblate magnetic fabric, suggesting an increasing flattening strain (Hrouda, 1993; Borradaile and Henry, 1997). Tectonic flattening of the YC rocks, as determined from field and microscopic observations, is therefore consistent with the overall scalar AMS data. Significantly different magnetic fabric parameters were shown by the NPC. The very little to none deformation observed in the different facies of this complex correlates with the much reduced values of anisotropy degree (López de Luchi et al., 2010) and the lack of a dominant ellipsoid shape. Non-negligible tectonic flattening, as inferred from AMS data, was only observed locally on sites of the NPC located very close to the borders of the pluton, which are likely related to flattening against the country rock wall during emplacement.

The spatial distribution of magnetic and field foliations and lineations (Fig. 4a and b) may help elucidating the processes associated with emplacement and deformation of the Yaminué and Navarrete complexes. Consistency of AMS axes with mesoscopic foliation determined in the field was generally observed, giving significant confidence to a widespread use of the AMS directional parameters to interpret the petrofabrics.

The large exposures of the YC in the western sector of the study area show a very flat foliation (Fig. 4a) with an apparent large scale folding around a N-S trending axis developing an antiform of over 10 km wave-length. In the northern exposures, the magnetic and field foliations trend systematically WNW-ESE with a variable but shallow dip towards NNE. Lineations in this area systematically plunge towards N or NE (Fig. 4b). The same foliation and lineation trends are present in the CVL exposures, although they tend to show greater dip and plunge angles (around 40° to 50°). A few sites, close to the eastern border of the CVL exposures, show foliation planes with somewhat higher dips and NW-SE to N-S trends. The few sites sampled on the TG, in the eastern sector of the area (Fig. 4a), also show

low angle foliation dips towards the North or East but with significant more scatter. Lineations are shallow and their directions range from North to East too.

The mineral and magnetic fabrics of the YC, TG and CVL are mainly the product of high-temperature deformation occurred during and after emplacement. The directional data presented in Figs. 4a and b suggest that these units were emplaced and subsequently deformed in a NNE-SSW compressional field, with YC attaining the highest deformation. Petrographic and AMS data clearly indicates that the CVL underwent a significantly lower deformation. However, similar foliation and lineation trends to those of the YC rocks strongly argue for the same regional stress field during intrusion of the CVL.

Exposures of the NPC in the western area are formed by the Robaina and the Guanacos facies. A general trend of foliation planes dipping towards the NE or E with low to intermediate angles and a systematic alignment of low

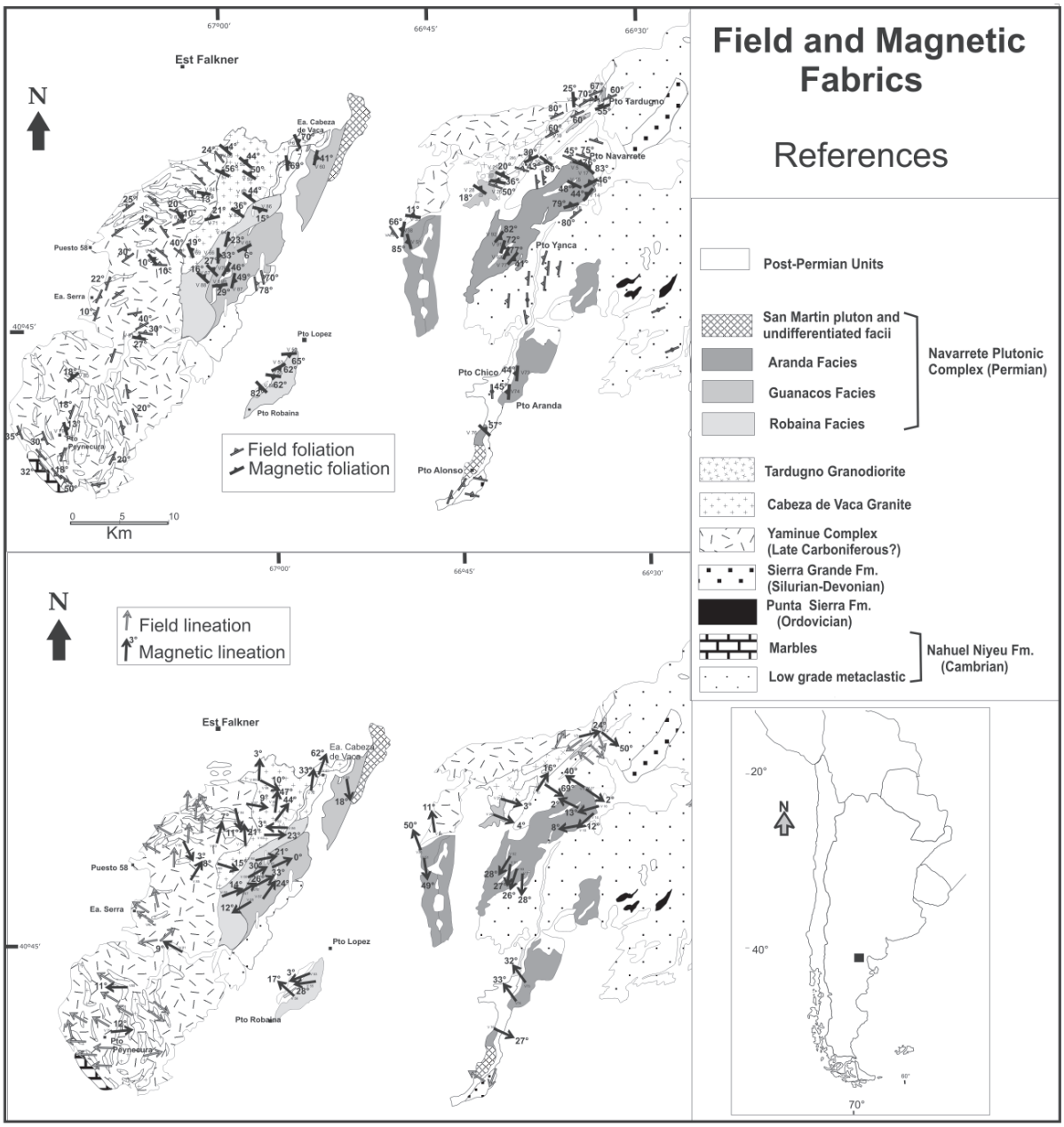

FIGURE 4 | **Structural and magnetic fabric directional data for the area west of Valcheta; A) Distribution of field and magnetic foliations; B) Distribution of field and magnetic lineations.**

angle k1 axes trending ENE are observed (Fig. 4 a,b). This suggests a far field NW-SE compressive stress during emplacement of these plutons. The eastern outcrops, on the other hand, are dominated by the Aranda facies. This is characterized by oblate fabrics and the orientation of the foliation planes seems to be mostly controlled by boundary effects. A flattening effect due to compression against the walls is confirmed in a few cases. A WNW-ESE to NW-SE far field maximum stress can be inferred during emplacement of the Aranda facies at least for some areas (west of Puesto Yanca, Fig. 4 a,b) where almost identical foliations and lineations are observed.

AMS and microstructural analyses indicate that the Late Paleozoic granitoids in the northeastern region of the North Patagonian Massif were intruded under two different tectonic regimes. The oldest units, i.e. the YC, TG and CVL, were intruded and subsequently deformed, in a NNE-SSW compressional stress field. A major change in the tectonic regime occurred before the intrusion of the large igneous bodies of the NPC, which are virtually free of solid state deformation. Mineral and magnetic fabrics of these bodies suggest that they were emplaced under a NW-SE to WNW-ESE far-field maximum stress.

GRAVITY SURVEY

Further insights into the crustal structure of the study region and the extension in depth of different igneous bodies, was gained through a gravity survey. One hundred and forty four topographic and gravity stations were surveyed in the study area (Fig. 5a). Gravity measurements were done with a LaCoste & Romberg gravity-meter, with ±0.01 mGal precision. All measurements were referred to the IGSN71 (Internacional Gravity Standarization Net 1971, Morelli et al., 1974). Sub-metric precision of altitude determination at each station was obtained by differential mode GPS recordings. Density measurements of the most representative lithologies (Table 2) were carried out in order to constrain the gravity models. Our survey was complemented with a previous regional gravity database of 1680 stations along NE Patagonia from the Instituto de Física de Rosario (Universidad Nacional de Rosario) and the Instituto Geofísico Sismológico “Ing. F. S. Volponi” (Universidad Nacional de San Juan). To identify the residual gravity anomalies (Fig. 5b).the regional gravity effect was substracted by a 35 km upward continuation of the Bouguer general anomaly map.

A central negative residual Bouguer anomaly extending from the Nahuel Niyeu village towards the SSW is observed in the map (Fig 5b). This anomaly coincides with the exposures of the eastern bodies of the NPC, the Flores granite and all mapped outcrops of the Silurian-Devonian unmetamorphosed sandstones of the Sierra Grande Formation. A large positive anomaly of up to 15 mgals coincides with the exposures of the YC and extends southwestward. Towards the eastern margin of the surveyed area another positive anomaly of around +5 mgals is observed. Table 2 shows that the YC and NPC have very similar densities. The NNF, on the other hand, is somewhat denser than all other lithologies. Therefore, no correlation is apparent between the residual Bouger anomalies and the densities of the exposed lithologic units. This suggests that the gravity signature is governed by deeper features and points to different structural levels being exposed in the region. Therefore, the western exposures, with the largest positive gravity anomaly, should correspond to significantly deeper levels than the central area.

The relationship between the gravity data and the basement structures was quantified with a 2D model (obtained with the SAKI program, Webring, 1985) of density distribution in the subsurface along cross-section A-B (see location in Fig.5b).

The model suggests that the exposed rocks in the western area correspond to crustal levels some 10 km deeper than those in the central area. This is consistent with supracrustal unmetamorphosed sedimentary rocks (Sierra Grande Fm.) and very low grade metamorphic units of the NNF only exposed in the latter area, and which coincide with the negative residual anomaly. The gravity model portrays the YC as a relatively thin unit, which is consistent with the subhorizontal foliations and field observations of interlayering of the deformed granitoids and the metasediments of the NNF that suggest YC as a shallow-dipping sheet or series of sheets.

TEXTURAL OBSERVATIONS AND GEOBAROMETRIC DATA

We used the Al-in hornblende geobarometer to obtain pressure of emplacement of the NPC and YC (Table 3). We measured major oxides in core-to-rim transects through hornblende and adjacent plagioclase. Data were taken from minerals in contact with quartz in order to fulfill the requirement of silica saturation. Technical details of determinations are presented in Table II (available in the electronic version of the paper at www.geologica-acta.com).

We used one sample of amphibole bearing biotite-tonalite from the central part of the YC and five samples of biotite-amphibole porphyritic tonalite to granodiorite of the NPC, i.e. three samples of the Guanacos facies and two of the Aranda facies (see location of samples in Fig. 3). Most of the data fulfill the criteria of hypersolidus equilibration and the ratio Fe/(Fe+Mg) for the amphiboles is always lower than 0.65 which agrees with the primary

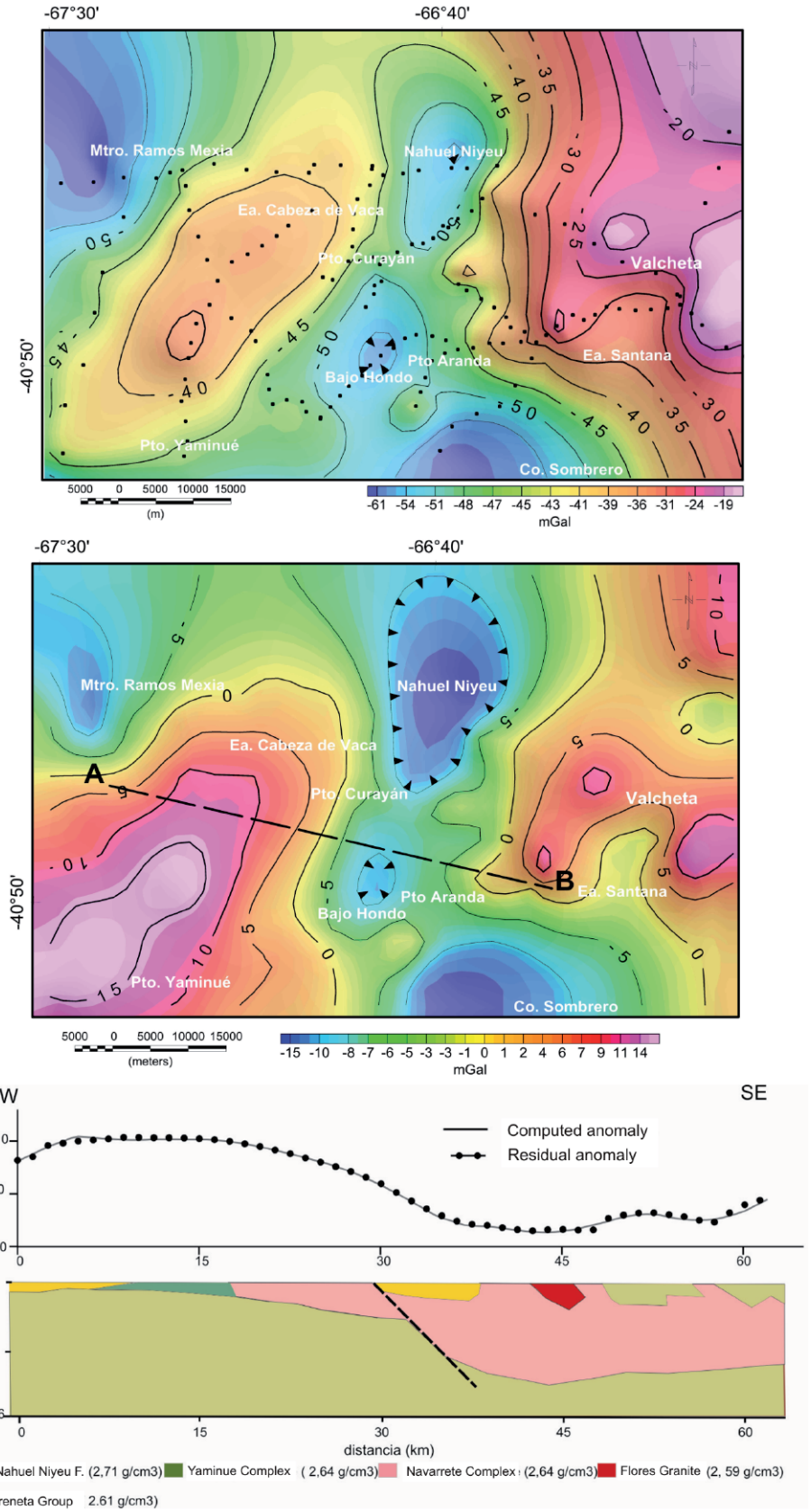

FIGURE 5 | **Gravimetric data for the area west of Valcheta: Top) Regional Bouguer anomaly map; center) Residual Bouguer anomaly map; bottom) Upper crustal model for cross-section A-B, based on the gravity and density data (Table 2).**

TABLE 2 | **Density of the main geological units exposed in the study area. N: number of individual calculations per site. Mean densities are shown with one standard deviation values. Location of samples is in Figure 4.**

Site	N	Density (x 10^3 Kg/m^3)	Mean density (x 10^3 Kg/m^3)
Nahuel Niyeu Formation			
V6	6	2.747	2.717 ± 0.028
V229	6	2.691	
V100	6	2.714	
Yaminué Complex			
V80	8	2.725	2.643 ± 0.057
V81	9	2.637	
V85	10	2.611	
V89	8	2.599	
Cabeza de Vaca Leucogranite			
V57	8	2.602	2.603± 0.003
V58	7	2.606	
V69	7	2.601	
Navarrete Plutonic Complex			
V17	7	2.625	2.643 ± 0.009
V53	8	2.660	
V66	7	2.614	
V68	7	2.649	
V74	7	2.655	
V77	7	2.654	
Flores Granite			
V23	7	2.603	2.593 ± 0.013
V42	8	2.584	

magnetite that characterizes these rocks (López de Luchi et al., 2010). High plagioclase anorthite content (outside the range An25-35) or low K-feldspar activities can increase the Al-in-hornblende independent from pressure, therefore the Al-in-hornblende thermobarometer was restricted to the plagioclase compositions ~ An25-40 (Anderson and Smith, 1995).

Sample V80 from the YC corresponds to a porphyritic biotite-tonalite with scarce hornblende that shows a uniform distribution, lacks resorption borders and is not armoured but intergrown with biotite, which indicates that it crystallized at the emplacement level. Data corresponds to pairs of cores or rims of both amphibole and normally zoned plagioclase. Crystallization temperatures and pressures obtained for V80 vary between 698-749°C (average 722 ± 27 °C) and 5.7-4.4 kbar (average 5.1 ± 0.6 kbar).

Complex magma mingling and mixing processes are indicated in the NPC (Guanacos and Aranda facies, López de Luchi et al., 2010). V65 corresponds to the dominant lithology of the Guanacos facies, while V65b belongs to an enclave. V65 is a coarse-grained grey hornblende-biotite tonalite. Zoned plagioclase grains are generally less than 1 cm in length and typically display a complex zoning with cores altered to sericite and epidote that show sharp boundaries with oligoclase limpid rims (López de Luchi et al., 2010). Uniform distribution of hornblende and the lack of armouring by biotite suggest in situ crystallization. Temperatures of 685-754 °C (average 726 ± 30°C) and pressure of 2.88-3.45 kbar (average 3.2 ± 0.3 kbar) were obtained using both core and rim pairs from V65. The enclave V65b shows temperatures between 709-745°C (average 730 ± 15°C) and crystallization pressure between 2.41 and 3.38 kbar (average 2.9 ± 0.4 kbar) that are within errors indistinguishable from those of the host V65. Sample V91 (Fig. 3) is a granodiorite of the Aranda facies without alteration and in sharp contact with a very low grade metaclastic facies of the NNF. Rock is a medium-grained and light pinkish grey biotite-hornblende granodiorite with a trend to porphyritic textures due to plagioclase megacrysts and with around 10% of mafic and opaque minerals (hornblende, biotite, titanite, zircon, apatite, allanite and magnetite). Amphibole is always armored by biotite and makes up elongate aggregates which indicate that it probably did not crystallize at the emplacement level. Zonation of plagioclase is complex and mostly oscillatory. The results show a complex crystallization history for this rock. The hornblende crystals generally appear to be normally zoned, suggesting higher pressures and temperatures of crystallization for the cores than for the rims If calculations are performed with the SiO_2 impoverished amphibole cores and the andesine (around 35%), core pressure varies between 4.77 and 5.80 kbar (average 5.3 ± 0.5 kbar) and temperatures between 717 and 748°C (average 729 ± 15°C). When the dominant oligoclase rims and small crystals of the matrix together with the more silica rich amphibole rims are used, temperatures of 754-723°C (average 738° ±15°C) and pressures between 2.55 and 3.25 kbar (average 2.9 ± 0.4 kbar) are obtained. As the textural observations indicate that the amphibole is set in an aggregate surrounded by biotite, this data does not correspond to the crystallization pressure of the host but probably indicates the pressure path of the ascending magma entraining more mafic components. We can assume a trajectory of ascent that started at least at around 5 kbar followed by an episode of crystallization at around 2.9 kbar.

An enclave (V74) was collected from the outcrops of the Aranda facies near Pto. Aranda (Fig. 3). Rocks are fine grained equigranular amphibole-biotite diorite to monzodiorite. Host rock for the enclave is a biotite-porphyritic granodiorite. Amphiboles of the enclave can be separated in 3 groups on the basis of the Si content. Different results are obtained considering which group is used in the calculations. Results range from 2.89-3.44 kbar (average 3.1 ± 0.3 kbar) and temperatures between 712-743ºC (average 727° ± 15°C), to 0.9-2.1 kbar (average 1.5 ± 0.5 kbar) and temperatures between 712-740ºC (average 725° ± 12°C). Within errors, pressure around 3.1 kbar is equivalent to the lower

TABLE 3 | **Emplacement depth calculated from the thermobarometry data for selected samples of the YC and NPC. Pressures were converted into emplacement depth on the assumption of an average crustal density of 2.8 g/cm³. See text for discussion. Location of samples is in Figure 3. See Appendix for the analytical major element results for the plagioclase and amphibole samples used in the calculations.**

	Sample	Rock type	Average P (kbar)	Depth (km)	Field observation
Western sector					
Yaminue Complex					
	V80	Granodiorite	5.1 ± 0.6	18 ± 2	Dominant lithology
Navarrete Plutonic Complex					
	Guanacos Facies				
	V65	Tonalite	3.2 ± 0.3	11 ± 1	Dominant lithology
	V65b	Monzodiorite	2.9 ± 0.4	10 ± 1	Enclave
Eastern sector					
Navarrete Plutonic Complex					
	Aranda Facies				
	V91	Granodiorite	5.3 ± 0.5	19 ± 2	Dominant lithology
			2.9 ± 0.4	10 ± 1	
	V74	Monzodiorite	3.1 ± 0.3	11 ± 1	Enclave
			1.5 ± 0.5	5 ± 2	
	Guanacos facies				
	VAL 221	Monzodiorite	2.1 ± 0.5	7 ± 2	Dominant lithology

calculated pressure for V91 and comparable with the western sector of the NPC.

VAL 221 (Fig. 3) is a fine to medium grained equigranular gray monzodiorite to diorite stock that exhibits sharp contact with the NNF. The hornblende crystals are normally zoned, meaning core to rim decrease in Al and Ti. Pressure is bracketed between 1.43-2.50 kbar (average 2.1 ± 0.5 kbar) and T ranges between 697 - 796 ºC (average 742 ± 50 ºC). These P-T constraints are interpreted as indicating the emplacement depth for this rock because amphibole is in textural equilibrium with the rest of the minerals. The diorite-monzodiorite represents a hybridization stage during the petrological evolution of NPC.

A crustal section across NNF indicates a decrease in the metamorphic grade from the easternmost outcrops near Valcheta towards the west (López de Luchi et al., 2008). This implies that if both the host of V74 and VAL 221 record a similar P, the contact between the very low grade facies of NNF with the green-schist facies intruded by the Ordovician granites should predate emplacement of NPC.

Pressures were converted into emplacement depth on the assumption of an average crustal density of 2.8 g/cm³ (Table 3). Because the uncertainty in pressure determinations using Anderson (1996) thermobarometer is ± 0.6 kbar, the corresponding uncertainty in emplacement depth would be ± 2.1 km. In any case, the significantly different emplacement levels obtained for the YC (around 18 km) and the NPC (around 10 km) are very consistent with the gravimetric model that suggests around 10 km of uplifting of the exposures of the YC with respect to the eastern outcrops of the NPC (Fig. 5b).

ISOTOPE DATA: SM-ND MODEL AGES

The Nd isotopic composition of igneous and metamorphic rocks allow investigating differences among magma production events and defining crustal provinces (Bennett and DePaolo, 1987). We revised, compiled and interpreted the already published and our own Nd isotopic data (Table 4) for Paleozoic to Lower Jurassic magmatic, sedimentary and metamorphic units of the northeastern corner of the NPM in order to evaluate their sources and petrological affinities.

Analytical Techniques and Sm-Nd parameters and Model Ages Calculation (T_{DM})

The ε_{Nd} notation is a parameter that compares the sample Nd isotope ratio ($^{143}Nd/^{144}Nd$) with the isotopic composition of the primitive mantle (CHUR) at a specific time. The most useful ε_{Nd} is that one calculated backwards, at the time of crystallization or metamorphism of the rock, because it can be used as a proxy of the magma source. There are two different ways of calculating model ages, a single stage model (Goldstein et al., 1984) that considers a linear evolution of the Nd isotopic composition and the two stage model (De Paolo et al., 1991) that takes into account the mixing of melts or sources in the petrogenetic processes. Choosing between the two available models is

TABLE 4 | **Sm-Nd isotopic data for the different units of NE North Patagonian Massif. Location of samples is in Figure 2. All Nd isotopic data were previously normalized against the value of 146Nd/144Nd = 0.7219 and Jolla Nd standards or equivalents by the corresponding authors. 1- this work, 2- Pankhurst et al. (2006), 3- Basei et al (2002), 3- Pankhurst et al. (1993).**

Locality	Unit	Rock type	Method	Age (Ma)	Sample	$f_{Sm/Nd}$	ε_{Nd} (t)	T_{DM} (Ga)
Sediments in Precambrian (?) – Cambrian basins								
Sierra Grande	El Jagüelito Fm.	Metasandstone	U-Pb Inh	~ 530 [2]	SGR-018 [2]	-0.38	-3.70	1.598
	Mina Gonzalito	Bt - Grt Gneiss	U-Pb	472 ± 15 [2]	GON-014 [2]	-0.37	-4.80	1.648
Valcheta	Nahuel Niyeu Fm.	Metasediment	U-Pb Inh	~ 515 [2]	V5A [1]	-0.37	-5.07	1.713
	Nahuel Niyeu Fm.	Metapelite	U-Pb Inh	~ 515 [2]	NIY-012 [2]	-0.40	-5.37	1.671
Ordovician granitic magmatism								
Sierra Grande	Arroyo Salado	Granite	U-Pb	475 ± 5 [2]	SGR-016 [2]	-0.34	-3.00	1.573
	Playas Doradas	Granite	U-Pb	476 ± 4 [2]	SGR-019 [2]	-0.38	-2.63	1.453
	Sierra Grande	Granite	U-Pb	476 ± 6 [2]	SGR-035 [2]	-0.38	-2.88	1.480
Eastern Colorado	Pichi Mahuida	Granodiorite	U-Pb	474 ± 6 [2]	PIM-113 [2]	-0.34	-4.66	1.736
River	Pichi Mahuida	Granite	U-Pb	475 ± 5 [2]	PIM-115 [2]	-0.24	-5.32	1.633
Carboniferous (?) syn-deformational granitic intrusions								
Valcheta	Yaminué Complex	Ortogneiss			V10 [1]	-0.34	-4.91	1.629
	Yaminué Complex	Foliated Granodiorite			AB110 [3]	-0.53	-5.80	1.534
	Yaminué Complex	Foliated Granodiorite			829A [3]	-0.34	-3.59	1.497
	Yaminué Complex	Tonalite	U-Pb	300 ± 6 [3]	V25 [1]	-0.43	-6.19	1.482
Permian post-deformational granitic intrusions								
Valcheta	Navarrete pluton	Granodiorite	U-Pb	281 ± 3 [2]	NIY-010 [2]	-0.36	-2.08	1.292
	San Martin pluton	Granodiorite	U-Pb	~ 267	MSM-063 [2]	-0.39	-5.38	1.486
Mesozoic granitic magmatism								
Valcheta	Treneta (?)	Porphyry quartz			NIY-011 [2]	-0.34	-3.74	1.413
	Flores	Granite	Rb-Sr	188 ± 3 [4]	V27 [1]	-0.56	-5.34	1.403

difficult because each model has its own advantages and inconveniences. The main failures of the single stage model are referred to the uncertainties that may result from the Sm/Nd fractionation of the granitic melts and their sources during partial melting, Sm/Nd fractionation during magma differentiation and the mixing of melts or sources during the petrogenetic processes. On the other hand, the two stage model assumes that all the sources follow the same isotopic evolution as the average continental crust (Wu et al., 2003) According to Wu et al. (2003), Jahn et al. (2000) and our own observations, and in order to minimize the error at the model ages, we choose to use the single stage model if $-0.3 \geq f_{Sm/Nd} \geq -0.5$, within the values of the $T_{DM1} \approx T_{DM2}$, and the two stage model if $-0.3 \leq f_{Sm/Nd}$ or $f_{Sm/Nd} \leq -0.5$. In order to establish criteria to compare the values, we recalculated all the available data under these assumptions. The obtained parameters (ε_{Nd}(t), $f_{Sm/Nd}$, T_{DM1} or T_{DM2} depending the case) are presented in Table 4. Mesoproterozoic (1.3-1.7 Ga) T_{DM} model ages and negative ε_{Nd} between -2 and -6 characterize all Paleozoic rocks in the study region. A detailed discussion of these results is presented in the next section.

DISCUSSION

The multidisciplinary studies carried out in the northeastern corner of the North Patagonian Massif described above provide significant constraints for the Paleozoic tectonic evolution of northern Patagonia. All available evidence can be reconciled in a tectonic model that portrays the NPM as a para-authochtonous block that underwent a late Paleozoic frontal collision with Gondwana. This evidence and details of this model are discussed below.

Evidence for a Late Paleozoic collision

Von Gosen (2003) proposed that a major NNE-SSW contractional event affected the northeastern sector of the NPM in the Late Paleozoic. He based his inference on top-to-the-SSW thrusts affecting the Sierra Grande and Nahuel Niyeu Formations south of the Nahuel Niyeu village, in the central area of our study region. According to this author this deformational event predated the intrusion of the Navarrete plutonic complex, now dated as Early Permian (281 Ma). After this, the regional stress field rotated counterclockwise to reach an approximate WNW-ESE direction by Late Permian times. Distribution of outcrops in the study area plus the results of the gravity survey and the geobarometric data indicate that exposures in the western sector (i.e. YC) correspond to a structural level some 10 km deeper than the one exposed in the central sector (i.e. Sierra Grande Fm., eastern outcrops of NPC). Microstructural and AMS results (Fig. 4) indicate that the tonalitic to granitic YC have undergone an intense tectonic high- and low-temperature deformation, characterized by homogeneous WNW trending foliations shallowly dipping towards the NNE and NNE trending subhorizontal lineations in its northern part. The CVL shows foliation trends parallel to those of the YC with moderate dip towards the NNE, but

with microstructures and magnetic fabrics suggestive of syn-magmatic to high temperature gentler deformation. The TG also shows evidence of high to low temperature tectonic deformation and foliation planes consistent with top to the SW thrusting (Von Gosen, 2003). The directional consistency of the shallow foliations and lineations in YC coupled with the microstructural analyses and gravity data clearly suggest a sheet-like geometry of the igneous bodies that were intruded and deformed during a main compressive event. Consistency of field and magnetic fabric foliations and lineations from the CVL and TG with those of YC, but with less intense deformation, can be explained by a later emplacement of the former units during the same tectonic episode, i.e. a major NNE-SSW thrusting event. Such scenario would explain the sheet-like nature of the plutons, the progressive deformation recorded by the different units, the homogeneous WNW-ESE shallow foliations and the shallowly dipping lineations trending N to NE. Our data can therefore be interpreted as a record of the same tectonic event described by Von Gosen (2003), but at deeper crustal levels. Therefore, evidence of a major NNE-SSW compressional event affecting this area in the Late Paleozoic looks robust. Age constraints on this event are not very precise. The Yaminué and Tardugno granitoids have been dated as ca. 300 Ma, but with large uncertainties (Table 1) and the CVL has not been dated yet. The main time constraint on this event is provided by the 281±3 Ma age of the NPC which is not affected by such deformation and for which field and magnetic fabrics are interpreted as evidence of intrusion under a NW-SE to WNW-ESE far field compressive stress.

The NNE-SSW compressional event affecting the rocks of the study area can be compared and correlated with the Late Paleozoic deformational event (Fig.1b) that folded and thrust-faulted the Sierra de la Ventana clastic deposits (Harrington, 1962; Buggisch et al., 1987; Japas, 1999; Ramos, 2008, and references therein). Paleomagnetic data from the youngest exposed unit of this succession (the Tunas Formation, Tomezzoli and Vilas, 1999; Tomezzoli, 2001) indicate that folding of the sequence took place mainly in the Early Permian, while sedimentation was still taking place (López Gamundi and Breitkreuz, 1997). Ar-Ar dating of an ash bed in the Tunas Fm. by Tohver et al. (2008) yielded 282.4±2.8 Ma. Vergence of folded structures in this region is to the NNE (see Ramos, 2008 and references therein).

A few hundred kilometers to the west of Sierra de la Ventana, in the province of La Pampa, the highly deformed granitoids of the Cerro Los Viejos (Fig. 1b) show a SSW dipping WNW trending foliation (Tickyj et al., 1999). Tomezzoli et al. (2003) published a magnetic fabric study of these highly deformed rocks that shows that the NNE-SSW major compressional stress was later superseded by a NW-SE directed stress as seen in the magnetic lineations and S-C surfaces. Radiometric ages suggest that the first deformational event may correspond to the biotite K-Ar ages of 304±15 and 330±15Ma (Linares et al., 1980), whereas younger ages of 280.4 ± 2.3; 261 ±13; 265 ± 13 Ma (Tickyj et al., 1999) may be related to the second event. Despite uncertainties, the structural evolution of the Cerro Los Viejos and the Yaminué-Navarrete areas are coeval and kinematically consistent. Ar-Ar ages on chlorite, biotite and muscovite from deformed basement rocks of the Sierra de la Ventana region around 265 Ma (Tohver et al., 2008) also suggest the possibility of two stages of deformation in the whole region: a NNE verging contractional thrust and fold belt followed by a WNW-ESE compressional event that may have resulted in further folding and/or transpressive deformation as proposed by Sellés Martinez (1989). The latter may have taken place along the WNW-ESE Pigué, Salitral de la Vidriera and Nueva Roma transcurrent fault systems (Bonorino et al., 1987; Alvarez, 2004).

In the three regions the first event took place around 300 Ma and corresponded to a contraction orthogonal to the boundary between Patagonia and the Gondwana blocks. The second event occurred between 280 and 260 Ma by a WNW-ESE contraction that may have produced NNE trending folds and faults and controlled the emplacement of large granitoid bodies in northern Patagonia, as the NPC. This later event is likely expressed in many areas as E-W block displacements and transpressive deformation. Gregori et al. (2008) have argued against the existence of a frontal collision between Patagonia and Gondwana and have proposed a single but heterogeneous tectonic event due to a variable compressive stress direction recorded along the North Patagonian Massif, governed by a major WNW-ESE transcurrent displacement between both tectonic blocks along the Huincul-Rio Colorado fault system. Robust evidence of successive, near orthogonal, regional stress fields as inferred from our study and others already mentioned, cannot be explained by Gregori et al.'s model. However inhomogeneities in deformation due to a variable structural grain of the basement, as proposed by these authors, is likely present.

Arguments in favor of a frontal collision between the NPM and Gondwana during the latest Carboniferous (ca. 300 Ma) are: structures resulting from orthogonal deformation with opposite vergence at both sides of the boundary between Patagonia and SW Gondwana, the development of a very thick fold-and-thrust belt in Sierra de la Ventana, a fore-deep basin generated due to tectonic stacking to the NE (Claromecó fore-deep, see Ramos, 1984, 2008), and the location of the study region several hundred kilometers away from the Phantalassic active margin (Hervé et al., 1987). This is basically the model proposed by Ramos (1984, 2008) and von Gosen (2002, 2003). In this model,

an ocean must have been consumed under the NPM before collision, which should have resulted in arc magmatism along the northern margin of Patagonia. Closure of the oceanic basin and cease of subduction must have produced a re-arrangement of the plate kinematics around SW Gondwana with its subsequent changes in the regional compressional fields. The already mentioned counterclockwise rotation (from NNE-SSW to WNW-ESE) during the Early Permian, could result from such plate reorganization. SW Argentina and central Chile were affected by a significant tectonic phase in the Early Permian (280-265 Ma) called the San Rafaelic phase (Azcuy and Caminos, 1987; Llambías and Sato; 1995; Llambías et al., 2003). This has generally been ascribed to a major change in the subduction processes along the western margin of South American Gondwana (Hervé et al., 1987; Mpodozis and Ramos, 1989; Rapalini and Vilas, 1991).

Crustal continuity between Patagonia and southwestern Gondwana

Several authors have argued against the collisional model (Dalla Salda et al., 1990; Rapalini, 1998; Gonzalez et al., 2001; Pankhurst et al., 2006). However, in most cases arguments concern the allochthonous or authochthonous nature of the Patagonian block rather than the existence or not of a collision along its northern boundary.

Rapalini (1998) advocated that Patagonia is autochthonous based on Devonian to Permian paleomagnetic poles from the NPM which are consistent with the coeval apparent polar wander path for Gondwana. However, the confidence limits of the paleomagnetic poles allow a nearly orthogonal separation of up to about 1500 km between NPM and Gondwana in the Devonian to Middle Carboniferous (Rapalini, 2005). This is illustrated in figure 6, in which two different paleogeographic reconstructions are presented for the Early Devonian, based on the reference paleomagnetic pole of Gondwana for such age (McElhinny and McFadden, 2000) and the available pole for the Sierra Grande Fm. (Rapalini, 1998). Available paleomagnetic data cannot discriminate between a paleogeographic model in which Patagonia remains in its present position respect to the South American blocks or another in which it is orthogonally displaced 1500 km from its northern boundary. Therefore, a small ocean between both land masses is not precluded by the paleomagnetic data. The nearly orthogonal separation required (Fig.6) suggests that if an ocean was closed in the Late Carboniferous, approximation of the Patagonian block must have been orthogonal to the Gondwana margin, consistent with the deformational evidence on both sides.

Similarities in detrital zircon ages between the Early Paleozoic metasedimentary units of the North Patagonian

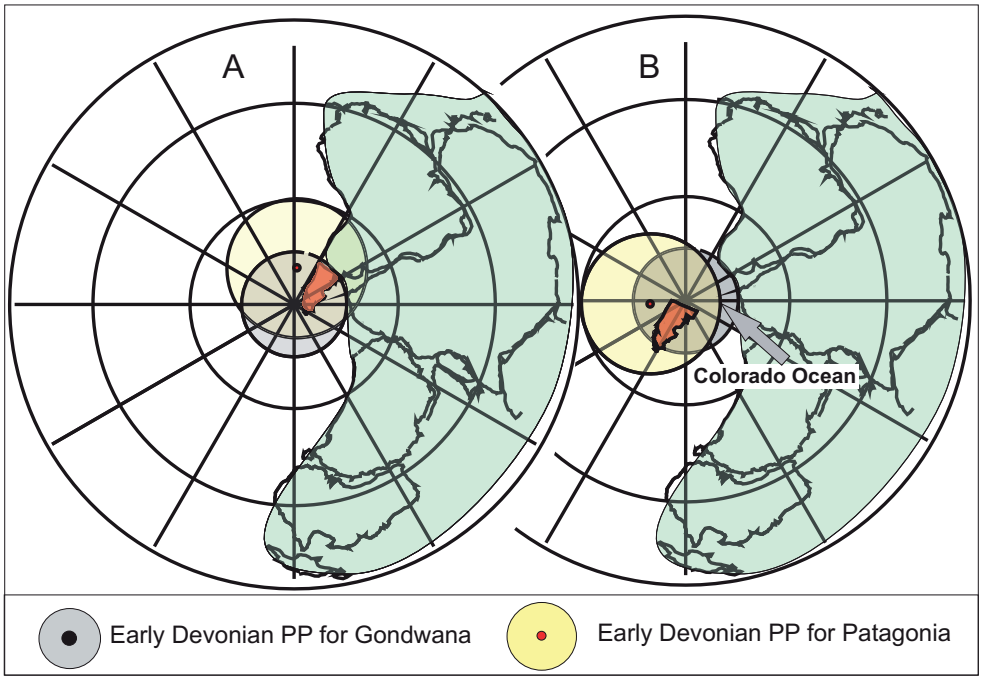

FIGURE 6 | **Paleogeographic reconstruction of Gondwana and Patagonia for the Early Devonian based on the mean paleomagnetic pole for Gondwana of such age as computed by McElhinny and Mcfadden (2000) and position of the Early Devonian paleomagnetic pole for the Sierra Grande Fm. (Rapalini, 1998). A) Patagonia remains attached to South America in its present position; B). Patagonia is displaced orthogonally to its northern boundary so that an ocean of approximately 1500 km exists between both land masses. Note that both A and B are paleomagnetically permissible reconstructions.**

Massif (Pankhurst et al., 2006) and some metasedimentary units of the Eastern Sierras Pampeanas, La Pampa province and the Puncoviscana basin (Schwartz and Gromet, 2004, Steenken et al., 2006, Rapela et al., 2007; Adams et al., 2008; Chernicoff et al., 2007, 2008 a,b) suggest similar sources for these basins. This makes an allochthonous origin for the NPM less likely. In particular maximum similarities are found in the age patterns of zircons from the late Cambrian- early Ordovician foreland basins of La Pampa with those of the metaclastic rocks of northeastern NPM (Fig. 7a).

Pankhurst and Rapela (1998) have proposed that a 2000 km long Early Ordovician magmatic arc (the Famatinian arc, e.g. Dahlquist et al., 2008) that extends along the southwestern margin of Gondwana is also found in the northeastern corner of the NPM (Pankhurst et al., 2006). This also suggests crustal continuity between northern Patagonia and Gondwana in the Early Ordovician (Fig. 1a).

Nd Isotopic evolution during the Paleozoic

In the NPM, the oldest crustal segment formed during the Late Paleoproterozoic, between 1.6 to 1.7 Ga (Table 4), is identified in the fine to medium-grained metasediments of Middle-Late Cambrian age exposed in the northeastern region. These low-grade metasedimentary units, El Jagüelito and Nahuel Niyeu Formations, show T_{DM} ages much older than their respective maximum depositional age (500-530 Ma), negative to slightly negative $\varepsilon_{Nd}(t)$ values (-5 to -4) and in all cases typical crustal values of $f_{Sm/Nd}$ (-0.37 to -0.4). This Late Paleoproterozoic bulk model ages and associated parameters indicate that there is no juvenile input in its consolidation as a rock, and hence nor in its precursor.

Ordovician granitoids intruding the low grade metaclastic units can be found in the northeastern NPM in two areas, west of Valcheta and Sierra Grande. Sm-Nd information is only available for the Arroyo Salado, Playas Doradas and Sierra Grande granites (Fig. 2) of the latter sector. These granites show T_{DM} model ages between 1.45-1.57 Ga (Table 4) and $\varepsilon_{Nd}(t)$ *ca* -2.7. Although all of them have a crustal signature, the Nd ages and the relatively more radiogenic $\varepsilon_{Nd}(t)$ suggest a juvenile melt supply to a bulk crustal segment.

Late Paleozoic magmatism is represented in the area by the YC and the NPC. The YC (Table 4, Fig 7b) exhibits T_{DM} values between 1.5 and 1.6 Ga, mean crustal $f_{Sm-Nd,}$n -0.34 to -0.53 and a spread of $\varepsilon_{Nd}(t)$ between -3.6 and -6.1. These values can typify either different degrees of recycling in the bulk crustal segment or different protoliths involved. However a main continental crustal recycling as demonstrated by the $\varepsilon_{Nd}(t)$ is inferred for all. The Permian magmatism represented by the NPC shows an episode of mixing of unequal parts of an old recycled crust with new inputs of a slightly depleted mantle-derived magma as demonstrated by the wide range in $\varepsilon_{Nd}(t)$ and T_{DM} ages between 1.3 and 1.6 Ga (Table 4, Fig. 7b). The calc-alkaline granodiorite of the Aranda facies at Pto. Navarrete (Figs. 2 and 3) show T_{DM} ages of 1.3 Ga and relatively radiogenic $\varepsilon_{Nd}(t)$ values (-2.08) suggesting a rejuvenation yielded by a new magma input to the already recycled bulk crustal segment.

The highly fractionated Lower Jurassic Flores Granite (table 4, Fig. 7a) exhibits T_{DM2} ages of 1.4 Ga and $\varepsilon_{Nd}(t)$ values of -5.3, which may imply the recycling of the younger bulk crust.

The Late Paleoproterozoic T_{DM} ages found in the NPM are very different from those of the Rio de la Plata craton (Fig. 7b) (see Steenken et al., 2004; Rapela et al., 2007), suggesting a significantly different Proterozoic crustal evolution. On the other hand, these model ages (Fig. 7b) are similar to those from the Sierras Pampeanas (Pampia terrane, Steenken et al., 2004) and the Arequipa-Antofalla block (Loewy et al., 2003, 2004) suggesting that the NPM might have a Proterozoic crustal connection with any or both of them.

Geotectonic considerations

If an ocean floor was consumed under northern Patagonia, previous to its frontal collision, a pre-collision arc-related magmatism should be found in this region. However, very little pre-280 Ma calc-alkaline magmatism has been reported from northern Patagonia. A relatively small "Colorado" ocean (Fig. 6B) that was consumed after a short-lived subduction may have produced scarce arc magmatism and can be an explanation for such absence. Varela et al. (2005) suggested that the less evolved (and normally more deformed) rocks of YC show a magmatic arc signature, whereas the more evolved terms fall into the syn-collisional fields in tectonic diagrams. The leucogranites of the CVL (Fig.3) are consistent with the final products of a collision (our own geochemical unpublished data). A geochemical and petrological change is observed in the NPC which has been interpreted as the product of a slab break-off process by Pankhurst et al. (2006).

Sm-Nd isotopic signature of rocks in the northeastern NPM suggest that during the Paleozoic the bulk crust was extensively recycled with two main episodes of juvenile addition to the bulk crustal segment: the first during Ordovician times as evidenced by granitic intrusions in the Sierra Grande area and the second during the lower Permian as shown by the data from the NPC.

All available evidence can be reconciled in a model that proposes a parautochthonous origin for the NPM (Rapalini, 2005; Ramos, 2008). Kinematic details of the evolution of

this terrane previous to its proposed collision are virtually unknown. Pankhurst et al. (2006) proposed that a collisional event affected the southwestern margin of the NPM in the Middle Carboniferous (ca. 325 Ma) in which the Deseado Massif was accreted. NPM was considered in this model an autochthonous part of Gondwana. Ramos (2008), on the other hand, suggested that the collision included the Antarctic Peninsula and southwestern areas of Patagonia, along a basically NW-SE subduction zone. Independent of the model, this collision apparently predated that at the northern margin of the NPM discussed in this paper. This older collision may have triggered a southward directed subduction under its northern margin and consumption of a small ocean basin.

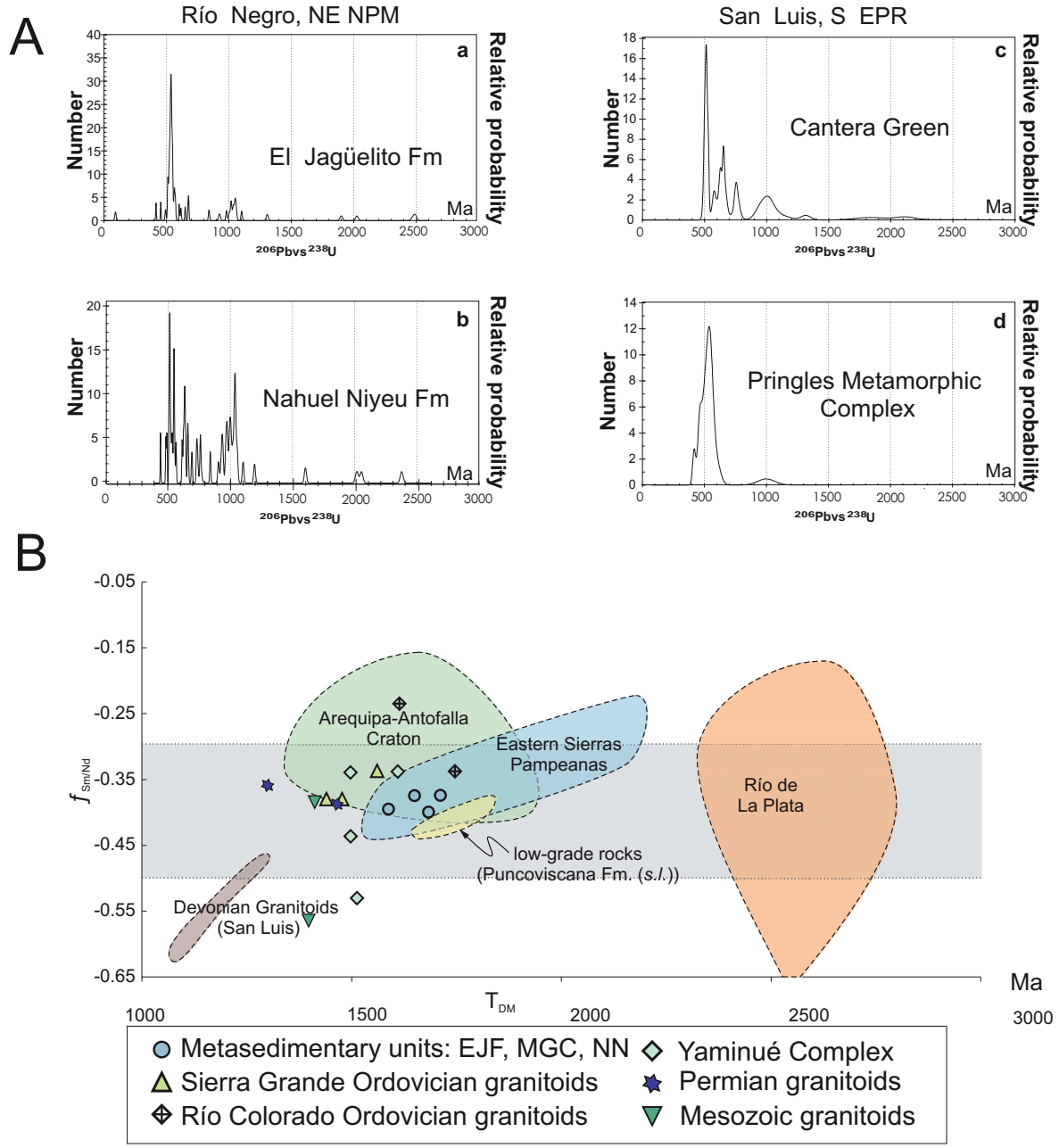

FIGURE 7 | **A) U-Pb zircon age patterns for metasedimentary samples from the a) El Jagüelito and b) Nahuel Niyeu Formations from the North Patagonian Massif and the c) Cantera Green and the d) Pringles Metamorphic Complex from Eastern Sierras Pampeanas. Data from Pankhurst et al. (2006), Steenken et al. (2006) and Chernicoff et al (2007). B) Correlation diagram showing the fractionation index fSm/Nd vs. the crustal residence time (TDM). Data from Table 4 and fields are taken from Steenken et al. (2004). The metasedimentary samples of the North Patagonian cover the range from 1.60 Ga to 1.71 Ga. The high TDM ages (<2.3 Ga) for the Rio de La Plata Craton exclude any primary connection with the North Patagonian Massif.**

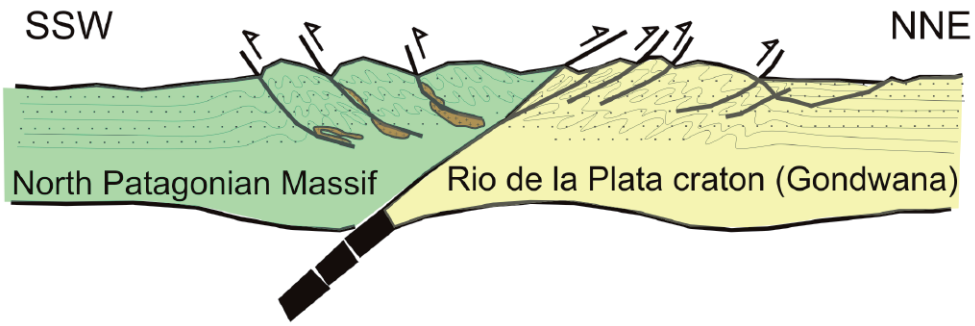

FIGURE 8 | **Sketch illustrating the opposite vergence of tectonic deformation due to a frontal collision between the North Patagonian Massif and the Río de la Plata craton (Gondwana) in Late Paleozoic times. The fold and thrust belt in the latter is best exposed in the Sierra de la Ventana and the Claromecó foredeep basin, whereas deformation in the former is seen in northeastern North Patagonian Massif. Note the presence of pre- to syn-collisional deformed magmatic bodies (modified from Ramos, 1984).**

The origin of this small "Colorado" ocean is not clear. It is possible that the NPM rifted away from basically the same relative position that occupied after its subsequent collision. In this case rifting might have evolved as a southward continuation of the Ordovician back-arc basin developed along most of the Famatinian magmatic arc. In the basement areas of La Pampa and San Luis provinces (Hauzenberger et al., 2001; Steenken et al., 2006; Chernicoff et al., 2007, 2008a; Zappettini et al., 2005) an early Ordovician back-arc basin was intruded by mafic rocks and closed and inverted in the Middle Ordovician due to the collision (Astini et al., 1995; Ramos, 2004) or approaching of the Laurentian Precordillera (Cuyania) terrane to the Gondwana margin (Steenken et al., 2006). The NPM, however, did not undergo such a collision as the southern boundary of the Cuyania terrane is located to the north (present coordinates) of the NPM. Plate kinematics re-organization after Cuyania collision may have induced further rifting along northern Patagonia that might have led to the small Colorado ocean. The late Silurian-Early Devonian clastic sedimentary rocks of the Sierra Grande Formation should represent the passive margin deposits on the southern margin of the ocean (see von Gosen, 2002). Closure of the ocean may have started in the Early or Middle Carboniferous, perhaps due to collision of the Deseado (Pankhurst et al., 2006) or the "Antonia" terrane (Antarctic Peninsula+southern Patagonia, Ramos, 2008). Problems with this model are the lack of rift-related sediments and magmatism. Some basic volcanic rocks intercalated in sedimentary rocks associated to the Sierra Grande Formation (Cortés, 1984) may be the only available evidence for such extensional magmatism. Such evidence, as it has been advocated for the later suture, may lay below several thousand meters of the Meso-Cenozoic infilling of the Colorado Basin.

An alternative to the model above is that the NPM rifted away from a location different to that of its subsequent collision. Assembly of Gondwana in the late Neoproterozoic and Early Paleozoic involved numerous tectonic blocks that rifted away and subsequently were accreted (Cawood, 2005). The possibility of the NPM to have originated close to or associated with other blocks (i.e., Pampia, Arequipa-Antofalla, Kalahari craton, the Antarctic Peninsula o Mary Bird Land) should be further investigated.

In the Late Carboniferous to Early Permian this small ocean was already consumed under the NPM and a frontal collision with the Gondwana passive margin took place. This event produced a major NNE-SSW compressive deformation with opposite vergences in the upper (SW) and the lower (NE) plates (Fig. 8). The collision of the parauthochtonous Patagonia probably triggered a major oceanic plate rearrangements in SW Gondwana that produced a nearly 90° counter-clockwise rotation of the regional stress field, that started to be governed by eastward (present-day coordinates) Panthalassic subduction beneath southern South America, that dominated northern Patagonia during most of the Permian.

SUMMARY AND CONCLUSIONS

A multidisciplinary study of Paleozoic magmatic rocks exposed in the northeastern corner of the North Patagonian Massif has shed light on its paleotectonic evolution.

Microstructural and magnetofabric studies have revealed the presence of two major suites of magmatic rocks. The Yaminué Complex and its associated units of the Tardugno Granodiorite and the Cabeza de Vaca leucogranites of late Carboniferous – earliest Permian age, were intruded and subsequently deformed under a strong NNE-SSW compressive stress associated to top-to-SW-thrust-tectonics, as also observed in unmetamorphosed supracrustal

sedimentary units in the same region. Similar deformation age and pattern have been observed in the Cerro los Viejos (La Pampa province) and the Sierra de la Ventana fold belt, both to the north of the Colorado basin, and the northern boundary of Patagonia. These latter areas, however, show a top-to-NE vergence of deformation as recorded in penetrative foliation in Cerro Los Viejos and widespread folding in Sierra de la Ventana. By the Early Permian (281 Ma) this deformational event had ceased and the regional stress field changed into a WNW-ESE maximum stress direction. Under these conditions, intrusion of the 281 Ma, and younger, Navarrete Plutonic complex took place as virtually undeformed granitoids.

Gravity surveys of our study area and geobarometric determinations clearly indicate a significant difference (around 10 km) in the exposed structural levels correspondent to the deformed granitoids of the Yaminué Complex and the thrusted and folded sedimentary successions of the Early Paleozoic Nahuel Niyeu and Sierra Grande Formations. Expression of the same deformational event at different crustal levels is therefore evident in this region.

A preliminary study plus a regional recopilation and recalculation of T_{DM} ages from the Early Cambrian metasedimentary units and the Paleozoic granitoids indicate a late Paleoproterozoic crustal signature for the NPM, which is similar to those found in the Sierras Pampeanas (Pampia terrane) and the Arequipa-Antofalla block. On the other hand, it is significantly different from the typical crustal ages of the Río de la Plata craton, suggesting that the latter was not connected with the NPM in the Proterozoic.

Similar detrital zircon age patterns between Early Paleozoic (meta) sedimentary rocks from the NPM and those from the Sierras Pampeanas (specially from La Pampa and San Luis) and the apparent continuation of the Early Ordovician Famatinian magmatic arc into northeastern Patagonia suggest crustal continuity between the Pampia and NPM blocks by the Early Paleozoic. Paleomagnetic data obtained so far from the NPM suggests that no wide ocean existed between Patagonia and Gondwana between the Devonian and Permian.

A geotectonic model is envisaged that supports the original proposition of Ramos (1984) of a frontal collision between the NPM and Gondwana in the Late Paleozoic. According to the available age constraints, this collision must have ended by the Early Permian (281 Ma). However, it must have been the final stage of a short-lived subduction process that consumed a small (< 1500 km) ocean under the NPM. A parauthochthonous origin of the NPM is therefore the simplest explanation for the available data. This block may have rifted away from the Pampia-Rio de la Plata blocks by the Early to Middle Paleozoic generating a small ocean that was consumed during the Carboniferous.

ACKNOWLEDGMENTS

This contribution is the product of a joint research project financed by the Agencia Nacional de Promoción Científica y Tecnológica (ANPCyT, Argentina) through grants PICT 2003 Redes 283, PICT 2005 Redes 33630 and PICT 2006 1074. Additional support by the University of Buenos Aires (UBACyT PIP X183), Universidad Nacional de San Juan (CICITCA- UNSJ. 2008-2009. Nº E816) and CONICET (Argentina) is acknowledged. Logistical support by the INGEIS (UBA-CONICET) and the Department of Geological Sciences (UBA) were of great importance for successful investigations. Many thanks go to the collaboration of R. Tomezzoli. C. Zaffarana, N. Celesia and A. D'Odorico participated during different field works. Dra. Ilka Schoenberg from the Department of Isotope Geology of the University of Goettingen performed the Sm-Nd measurements. José González del Tánago (Complutense University of Madrid) as well as the technician Alfredo Fernández are specially thanked for their assistance with use of the electron microprobe. Discussions and suggestions by C. Rapela, R. Pankhurst, V. Ramos, E. Tohver, P. Cawood, D. Gregori, J. Kostadinoff, among others, are gratefully acknowledged. Thorough reviews by C. Rapela, A.E.F.Costa, M. Garcés and an anonymous reviewer highly improved the quality of the final version.

REFERENCES

Adams, Ch., Miller, H., Toselli, A.J., 2008. The Puncoviscana Formation of northwest Argentina: U-Pb geochronology of detrital zircons and Rb-Sr metamorphic ages and their bearing on its stratigraphic age, sediment provenance and tectonic setting. *Neues Jahrbuch für Geologie und Paläontologie*, 247(3), 341-352.

Álvarez, G.T., 2004. Cuencas paleozoicas asociadas a la prolongación norte del sistema de Sierras de Ventania, provincia de Buenos Aires. Unpublished Doctoral Thesis. Bahía Blanca (Argentina), Universidad Nacional del Sur, 163pp.

Anderson, J.L., 1996. Status of thermobarometry in granitic batholiths. Transactions of the Royal Society of Edinburgh, 87, 125-138.

Anderson, J.L., Smith, D.R., 1995. The effects of temperature and fo_2 on the Al-in hornblende barometer. American Mineralogist, 80, 549-559.

Astini, R.A., Benedetto, J.L., Vaccari N.E., 1995. The Early Paleozoic evolution of the Argentine Precordillera as rifted, drifted and collided terrane: a geodynamic model. Geological Society of America Bulletin, 107, 253-273.

Azcuy, C.L., Caminos, R., 1987. Diastrofismo. In: Archangelsky, S. (ed.). El Sistema Carbonífero en la República Argentina. Academia Nacional de Ciencias Córdoba, 239-251.

Basei, M.A.S., Varela, R., Sato, A.M., Siga Jr., O., Llambías, E.J., 2002. Geocronología sobre rocas del Complejo Yaminué, Macizo Norpatagónico, Río Negro, Argentina. In: Cingolani, C.A., Cabaleri, N., Linares, E., López de Luchi, M.G., Ostera, H.A., Panarello, H.O. (eds.). El Calafate, 15th Congreso Geológico Argentino, Actas III, 117-122.

Bennett, V.C., DePaolo, D.J., 1987. Proterozoic crustal history of the western United States as determined by neodymium isotopic mapping. Geological Society of America Bulletin, 99, 674-685.

Bonorino, A.G., Kostadinoff, J., Schillizzi, R., 1987. Geofísica y geología del sector noroccidental de la cuenca del Colorado, provincia de Buenos Aires. Geoacta, 17, 167-177.

Borradaile, G.J., Henry, B., 1997. Tectonic applications of magnetic susceptibility and its anisotropy. Earth Science Reviews, 42, 49-93.

Bouchez, J.L., Delas, C., Gleizes, G., Nédélec, A., 1992. Submagmatic microfractures in granites. Geology, 20, 35-38.

Buggisch, W., 1987. Stratigraphy and very low grade metamorphism of the Sierras Australes of the Province of Buenos Aires, Argentina and implications in Gondwana correlations. Zentralblatt Mineralogie Geologie Paläontologie, 1, 819-837.

Caminos, R., 1983. Descripción Geológica de las Hojas 39g, Cerro Tapiluke y 39h, Chipauquil, provincia de Río Negro. Buenos Aires, Servicio Geológico Nacional, unpublished.

Caminos, R., 2001. Hoja Geológica N 4166-I Valcheta, provincia de Río Negro. Buenos Aires, Servicio Geológico Minero Argentino, Boletín 310, 78pp.

Caminos, R., Llambías, E.J., 1984. El basamento cristalino. In: Ramos, V.A. (ed.). Geología y Recursos Naturales de la provincia de Río Negro. Buenos Aires, 9th Congreso Geológico Argentino, Relatorio, 37-63.

Caminos, R., Chernicoff, C., Varela, R., 1994. Evolución tectónico-metamórfica y edad del Complejo Yaminué, Basamento pre-andino norpatagónico, República Argentina. 7th Congreso Geológico Chileno, Concepción, Actas II, 1301-1305.

Cawood, P.A., 2005. Terra Australis orogen: Rodinia breakup and development of the Pacific and Iapetus margins of Gondwana during the Neoproterozoic and Paleozoic. Earth-Science Reviews, 69, 249-279.

Chernicoff, C.J., Caminos, R., 1996a. Estructura y relaciones estratigráficas de la Formación Nahuel Niyeu, Macizo Norpatagónico oriental, Provincia de Río Negro. Revista de la Asociación Geológica Argentina, 51, 201-212.

Chernicoff, C.J., Caminos, R., 1996b. Estructura y metamorfismo del Complejo Yaminué, Macizo Norpatagónico oriental, provincia de Rio Negro. Revista de la Asociación Geológica Argentina, 51, 107-118.

Chernicoff, C.J., Zappettini, E., 2003. Delimitación de los terrenos tectono-estratigráficos de la región centro-austral argentina: evidencias aeromagnéticas. Revista Geológica de Chile, 30(2), 299-316.

Chernicoff, C.J., Santos, J.O.S., Zappettini, E.O., McNaughton, N.J., 2007. Esquistos del Paleozoico inferior en la Cantera Green (35°04'S- 65°28'O), sur de San Luis: Edades U-Pb Shrimp e implicancias geodinámicas. Revista de la Asociación Geológica Argentina, 62(1), 154-158.

Chernicoff, C.J., Zappettini, E.O., Santos, J.O.S., Griffin, W., McNaughton, N.J., 2008a. Foreland basin deposits associated with Cuyania accretion in La Pampa Province, Argentina. Gondwana Research, 13(2), 189-203.

Chernicoff, C.J., Santos, J.O.S., Zappettini, E.O., McNaughton, N.J., 2008b. Zircon U-Pb shrimp dating of lower paleozoic paraschists at sierra de Lonco Vaca, La Pampa province argentina. In: Linares, E., Cabaleri, N.G., Do Campo, M.D., Ducós, E.I., Panarello, H.O. (eds.). Book of Abstracts. San Carlos de Bariloche, VI South American Symposium on Isotope Geology, Abstracts, 65.

Cortés, J.M., Caminos, R., Leanza, H.A., 1984. La cobertura sedimentaría eopaleozoica. San Carlos de Bariloche, 9th Congreso Geológico Argentino, Relatorio, 65-84.

Dahlquist, J.A., Pankhurst, R.J., Rapela, C.W., Galindo, C., Alasino, P., Fanning, C.M., Saavedra, J., Baldo, E., 2008. New SHRIMP U-Pb data from the Famatina Complex: constraining Early-Mid Ordovician Famatinian magmatism in the Sierras Pampeanas, Argentina. Geologica Acta, 6(4), 319-333.

Dalla Salda, L., Cingolani, C., Varela, R., 1990. The origin of Patagonia. Comunicaciones, Una revista de geología andina, 41, 55-61.

De Paolo, D.J., Linn, A.M., Schubert, G., 1991. The Continental Crustal Age Distribution Methods of Determining Mantle Separation Ages From Sm-Nd Isotopic Data and Application to the Southwestern United States. Journal of Geophysical Research, 96(B2), 2071-2088.

Goldstein, S.L., O'Nions, R.K., Hamilton, P.J., 1984. A Sm-Nd isotopic study of atmospheric dusts and particulates from major river systems. Earth and Planetary Science Letters, 70, 221-236.

González, P.D., Poiré, D.G., Varela, R., 2002. Hallazgo de trazas fósiles en la Formación El Jagüelito y su relación con la edad de las metasedimentitas, Macizo Norpatagónico Oriental, provincia de Río Negro. Revista de la Asociación Geológica Argentina, 57(1), 35-44.

Gozálvez, M.R., 2009. Petrografía y edad $^{40}Ar/^{39}Ar$ de leucogranitos peraluminosos al oeste de Valcheta. Macizo Norpatagónico (Río Negro). Revista de la Asociación Geológica Argentina, 64, 183-359

Gregori, D.A., Kostadinoff, J., Strazzere, L., Raniolo, A., 2008. Tectonic significance and consequences of the Gondwanide orogeny in northern Patagonia, Argentina. Gondwana Research, 14(3), 429-450.

Harrington, H.J., 1962. Paleogeographic development of South America. American Association of Petroleum Geologists, Bulletin, 46(10), 1773-1814.

Hauzenberger, Ch., Mogessie, A., Hoinkes, G., Felfernig, A., Bjerg, E., Kostadinoff, J., Delpino, S., Dimieri, L., 2001. Metamorphic evolution of the Sierras de San Luis, Argentina: granulite facies metamorphism related to mafic intrusions. Mineralogy and Petrology, 71(1-2), 95-126.

Hervé, F., Godoy, E., Parada, M.A., Ramos, V., Rapela, C.W, Mpodozis, C., Davidson, J., 1987. A general view on the Chilean-Argentine Andes, with emphasis on their early history. In: Monger, J., Francheteau, J. (eds.). Circum-Pacific Orogenic Belts and Evolution of the Pacific Basin. Geodynamics Series, American Geophysical Union, Geological Society of America, 18, 97-113.

Hrouda, F., 1993. Theoretical models of magnetic anisotropy to strain relationship revisited. Physics of the Earth and Planetary Interiors, 77**,** 237-249.

Jahn, B.M., Wu, F.Y., Chen, B., 2000. Massive granitoid generation in Central Asia: Nd isotope evidence and implication for continental growth in the Phanerozoic. Episodes, 23(2), 82-92.

Japas, M.S., 1999. Revisión de las teorías acerca del arco de las Sierras Australes de Buenos Aires. Revista de la Asociación Geológica Argentina, 54(1), 9-22.

Jarosewich, E.J., Nelen, J.A., Norberg, J.A, 1980. Reference samples for electron microprobe analysis. Geostand. Newsl, 4, 43-47.

Jelinek, V., 1978. Statistical processing of magnetic susceptibility measured in groups of specimens. Studia Geophysical Geodynamics, 22, 50-62.

Kostadinoff, J., Gregori, D.A., Raniolo, A., 2005. Configuración geofísica-geológica del sector norte de la provincia de Río Negro. Revista de la Asociación Geológica Argentina, 60, 368-376.

Leanza, A.F., 1958. Geología Regional. In: Peuser (ed.). La Argentina, Suma de Geografía. Buenos Aires, 1(3), 217-349.

Linares, E., Llambías, E.J., Latorre, C.O., 1980. Geología de la provincia de La Pampa, República Argentina y geocronología de sus rocas metamórficas y eruptivas. Revista de la Asociación Geológica Argentina, 35(1), 87-146.

Llambías, E.J., Sato, A.M., 1995. El Batolito de Colanguil: transición entre orogénesis y anorogénesis. Revista de la Asociación Geológica Argentina, 50, 111-131.

Llambías, E.J., Varela, R., Basei, M., Sato, A.M., 2002. Deformación y metamorfismo neopaleozoico en Yaminué, Macizo Norpatagónico (40°50'S/67°40'W): su relación con la Fase Orogénica San Rafael y el arco de las Gondwánides. In: Cabaleri, N., Cingolani, C.A., Linares, E., López de Luchi, M.G., Ostera, H.A., Panarello H.O. (eds.). El Calafate, Actas 15th Congreso Geológico Argentino. Buenos Aires, Asociación Geológica Argentina, 3, 123-128.

Llambías, E.J., Quenardelle, S., Montenegro T., 2003. The Choiyoi Group from central Argentina: a subalkaline transitional to alkaline association in the craton adjacent to the active margin of the Gondwana continent. Journal of South American Earth Sciences, 16, 243-257.

Loewy, S., Connelly, J.N., Dalziel, I.W.D., Gower, C.F., 2003. Eastern Laurentia in Rodinia: Constraints from whole-rock Pb and U-Pb geochronology. In: Sircombe, K.N., McElhinny, M.W. (eds.). Orogenic belts, regional and global tectonics: A memorial volume to Chris McAulay Powell. Tectonophysics, 375, 169-197.

Loewy, S.L., Connelly, J.N., Dalziel, I.W.D., 2004. An orphaned basement block: The Arequipa-Antofalla Basement of the central Andean margin of South America. Geological Society of America Bulletin, 116(1-2); 171-187.

López de Luchi, M.G., Wemmer, K., Rapalini, A.E., 2008. The cooling history of the North Patagonian Massif: first results for the granitoids of the Valcheta area, Río Negro, Argentina. In: Linares, E., Cabaleri, N.G., Do Campo, M.D., Ducós, E.I., Panarello, H.O. (eds.). Book of Abstracts, VI South American Symposium on Isotope Geology, San Carlos de Bariloche, Abstracts, 33.

López de Luchi, M.G., Rapalini, A.E., Tomezzoli, R.N., 2010. Magnetic Fabric and Microstructures of Late Paleozoic granitoids from the North Patagonian Massif: Evidence of a collision between Patagonia and Gondwana? Tectonophysics, in press.

López Gamundi, O.R., Breitkreuz, C., 1997. Carboniferous to Triassic evolution of the Panthalassan margin in southern South America. In: López Dickins, J.M. (ed.). LatePaleozoic and Early Mesozoic events and their Global Correlation. Cambridge University Press, 8-19.

Manceñido, M.O., Damborenea, S.E, 1984. Megafauna de Invertebrados paleozoicos y mesozoicos. San Carlos de Bariloche, Relatorio del 9th Congreso Geológico Argentino, 413-465.

McElhinny, M.W., McFadden, P.L., 2000. Paleomagnetism. Continents and Oceans. London, Academic Press, Internat, Geophysics Series, 73, 386pp.

McGuire, A.V., Francis, C.A., Diar, M.D., 1992. Mineral standards for electronmicroprobe analysis of oxygen. American Mineralogist, 77, 1087-1091.

Morelli, C., Gantar, C., Honkasalo, T., Mc Connell, R.K., Tanner, J.G., Szabo, B., Uotila, U., Whalen, C.T., 1974. The International Gravity Standardization Net 1971 (I.G.S.N.71). International Association of Geodesy, 4(Special Publication), 194pp.

Mpodozis, C., Ramos, V.A., 1989. The Andes of Chile and Argentina. In: Ericksen, G.E., Cañas Pinochet, M.T., Relnemund, J.A. (eds.). Geology of the Andes and its relation to hydrocarbon and mineral resources. Circum-Pacific Council for Energy and Mineral Resources, Houston (Texas), Earth Science Series, 11, 59-90.

Pankhurst, R.J., Rapela, C.W. (eds.), 1998. The Proto-Andean margin of Gondwana. Geological Society of London Special Publication, 142, 383pp.

Pankhurst, R.J., Caminos, R., Rapela, C.W., 1993. Problemas geocronológicos de los granitoides gondwánicos de Nahuel Niyeu, Macizo Norpatagónico. Mendoza, 12th Congreso Geológico Argentino, 4(Actas), 99-104.

Pankhurst, R.J., Rapela, C.W., Fanning, C.M., Márquez, M., 2006. Gondwanide continental collision and the origin of Patagonia. Earth-Science Reviews, 76, 235-257.

Ramos, V.A., 1984. Patagonia: ¿Un continente paleozoico a la deriva? San Carlos de Bariloche, 9th Congreso Geológico Argentino, 2(Actas), 311-325.

Ramos, V.A., 2002. Evolución tectónica. In: Haller, M.J. (ed.). Geología y Recursos Naturales de Santa Cruz. El Calafate, 15th Congreso Geológico Argentino, Relatorio, 365-387.

Ramos, V.A., 2004. Cuyania, an exotic block to Gondwana: Review of a historical success and the present problems. Gondwana Research, 7(4), 1009-1026.

Ramos, V.A., 2008. Patagonia: a Paleozoic continent adrift? Journal of South American Earth Sciences, 26(3), 235-251.

Rapalini, A.E., 1998. Syntectonic magnetization of the Mid-Paleozoic Sierra Grande Formation. Further constraints for the tectonic evolution of Patagonia. Journal of the Geological Society of London, 155, 105-114.

Rapalini, A.E., 2005. The accretionary history of southern South America from the latest Proterozoic to the late Paleozoic: some paleomagnetic constraints. In: Vaughan, A.P.M., Leat, P.T., Pankhurst, R.J. (eds.). Terrane processes at the margins of Gondwana. London, Geological Society of London, 246(Special Publication), 305-328.

Rapalini, A.E., Vilas, J.F., 1991. Preliminary paleomagnetic data from the Sierra Grande Formation: Tectonic consequences of the first mid-Paleozoic paleopoles from Patagonia. Journal of South American Earth Sciences, 4(1-2), 25-41.

Rapela, C.W., Caminos, R., 1987. Geochemical characteristics of the Upper Paleozoic magmatism in the eastern sector of Northpatagonian Massif. Revista Brasileira de Geociencias, 17(4), 535- 543.

Rapela, C.W., Pankhurst, R.J., Casquet, C., Fanning, C.M., Baldo, E.G., González-Casado, J.M., Galindo, C., Dahlquist, J., 2007. The Río de la Plata craton and the assembly of SW Gondwana. Earth-Science Reviews, 83, 49-82.

Schwartz, J.J., Gromet, L.P., 2004. Provenance of a late Proterozoic-early Cambrian basin, Sierras de Córdoba, Argentina. Precambrian Research, 129, 1-21.

Sellés Martínez, J., 1989. The structure of Sierras Australes (Buenos Aires Prov. Argentina) An example of folding in a transpressive environment. Journal of South American Earth Sciences, 2(4), 317-329.

Steenken, A., Werner, K., López de Luchi, M.G., Siegesmund, S., Pawlig, S., 2004. Crustal Provenance and Cooling of the Basement Complexes of the Sierra de San Luis: An Insight Into the Tectonic History of the Pro to-Andean Margin of Gondwana. Gondwana Research, 7(4), 1171-1195.

Steenken, A., Siegesmund, S., López de Luchi, M.G., Wemmer, K., Frei, R., 2006. Neoproterozoic to Early Palaeozoic events in the Sierra de San Luis: Implications for the Famatinian geodynamics in the Eastern Sierras Pampeanas (Argentina). Journal Geological Society of London, 163, 965-982.

Tarling, D.H., Hrouda, F., 1993. The magnetic anisotropy of rocks. London, Chapman and Hall, 232pp.

Tickyj, H., Dimieri, L.V., Llambías, E.J., Sato, A.M., 1997. Cerro Los Viejos (38° 28'S - 64° 26'O): Cizallamiento dúctil en el sudeste de La Pampa. Revista de la Asociación Geológica Argentina, 52(3), 311-321.

Tickyj, H., Basei, M.A.S., Sato, A.M., Llambías, E.J., 1999. U-Pb and K-Ar ages of Pichi Mahuida group, crystalline basement of south-eastern La Pampa province, Argentina. Córdoba (Argentina), 2nd South American Symposium on Isotope Geology, Actas, 139-142.

Tohver, E., Cawood, P.A., Rossello, E.A., Riccomini, C., 2007. Demise of the Gondwana ice sheet in SW Gondwana: time constraints from U-Pb zircon ages. Santiago, Universidad de Chile, Geosur 2007, An International Congress on the Geology and Geophysics of the Southern Hemisphere, 163 (Abstract volume), 139-142.

Tohver, E., Cawood, P.A., Rossello, E., López de Luchi, M.G., Rapalini, A., Jourdan, F., 2008. New SHRIMP U-Pb and $^{40}Ar/^{39}Ar$ constraints on the crustal stabilization of southern South America, from the margin of the Rio de Plata (Sierra de Ventana) craton to northern Patagonia. American Geophysical Union, Fall Meeting, EOS(Abstract), T23C-2052.

Tomezzoli, R.N., 2001. Further palaeomagnetic results from the Sierras Australes fold and thrust belt, Argentina. Geophysical Journal International, 147, 356-366.

Tomezzoli, R.N., Vilas, J.F., 1999. Paleomagnetic constraints on the age of deformation of the Sierras Australes thrust and fold belt, Argentina. Geophysical Journal International, 138, 857-870.

Tomezzoli, R.N., MacDonald, W.D., Tickyj, H., 2003. Composite magnetic fabrics and S-C structure in granitic gneiss of Cerro de los Viejos, La Pampa province, Argentina. Journal of Structural Geology, 25(2), 159-169.

Uliana, M.A., Biddle, K.T., 1987. Permian to Late Cenozoic evolution of Northern Patagonia: main tectonic events, magmatic activity and depositional trends. In: McKenzie, G.D. (ed.). Gondwana Six: Structure, Tectonics and Geophysics. Washington, American Geophysical Union, Geophysical Monograph, 40, 271-286.

Uriz, N.J., Cingolani, C.A., Chemale, F.Jr., Armstrong, R.A., 2008a. U-Pb detrital zircon data from the Paleozoic Sierra Grande formation, North Patagonian Massif, Argentina. In: Linares, E., Cabaleri, N.G., Do Campo, M.D., Ducós, E.I., Panarello, H.O. (eds.). Books of Abstracts. San Carlos de Bariloche, VI South American Symposium on Isotope Geology, Abstracts, 162.

Uriz, N.J., Cingolani, C.A., Chemale Jr.F., Macambira, M.J., 2008b. Edades U-Pb en circones detríticos del Grupo Ventana (Provincia de Buenos Aires) y de la Formación Sierra Grande (Macizo Nordpatagónico): Análisis comparativo de Procedencia. San Salvador de Jujuy, 17th Congreso Geológico Argentino, Abstracts, 912-914.

Varela, R., Llambías, E.J., Basei, M.A.S., 2005. Caracterización química y geotectónica del Complejo Yaminué, basamento cristalino del Macizo Norpatagónico. La Plata, Congreso Geológico Argentino, 1(Actas), 377-384.

Vaughan, A.P.M., Pankhurst, R.J., 2008. Tectonic overview of the west Gondwana margin. Gondwana Research, 13, 150-162.

von Gosen, W., 2002. Polyphase structural evolution in the northeastern segment of the North Patagonian Massif (southern Argentina). Journal of South American Earth Sciences, 15, 591-623.

von Gosen, W., 2003. Thrust tectonics in the North Patagonian massif (Argentina): implications for a Patagonian plate. Tectonics, 22 (1), 1005, 33pp. doi:10.1029/2001TC901039.

Webring, M., 1985. SAKI: A Fortran program for generalized linear inversion of gravity and magnetic profiles. United States Geological Survey, 85-122(Open File Report), 108pp.

Wu, F.Y., Jahn, B.M., Wilde, S.A., Lo, C., Yui, T.F., Lin, Q., Ge, W.C., Sun, D.Y., 2003. Highly fractionated I-type granites in NE China (II): isotopic geochemistry and implications for crustal growth in the Phanerozoic. Lithos, 67, 191-204.

Zanettini, J.C., 1981. La Formación Sierra Grande (Provincia de Rio Negro). Revista de la Asociación Geológica Argentina, 36, 160-179.

Zappettini, E.O., Chernicoff, C.J., Villar, M.L., 2005. La faja de metagabros de La Pampa: evidencias geoquímicas y petrológicas de un magmatismo de retroarco en la región centro-austral argentina. La Plata, 16th Congreso Geológico Argentino, Actas III, 45-52.

Manuscript received October 2009;
revision accepted February 2010;
published Online July 2010.

ELECTRONIC APPENDIX

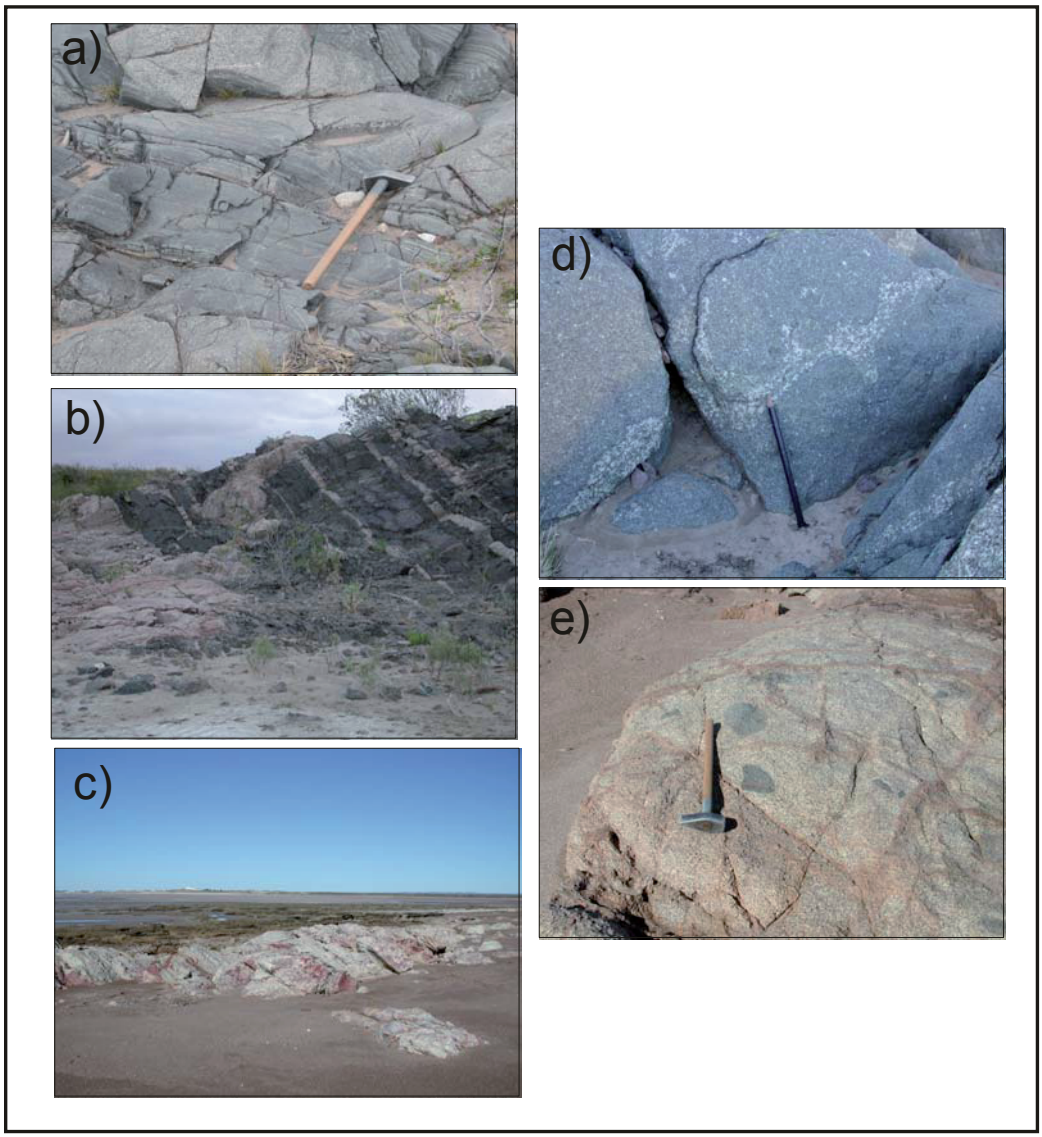

FIGURE 1 | **Field relationships of the Ordovician granitoids and their host and cover in the Sierra Grande Area of northeastern Patagonia. In the Sierra Grande area the host is the low grade metaclastic of the El Jagüelito Fm. and the cover corresponds to the clastic Sierra Grande Fm. a) Clear-cut contact between Arroyo Salado granodiorite and the El Jagüelito Fm near along the Arroyo Salado b) Clear-cut and cross-cutting contact between a granitic facies of the Arroyo Salado pluton and the El Jagüelito Fm. Thin sheets of the granite are emplaced also parallel to the pre-existing metamorphic fabric c) View of the erosional unconformity between Playas Doradas pluton and the Sierra Grande Fm. d) Small load-casts at the base of a more mafic facies. Granodiorite has concentrated between convex-downward lobes, and veins have risen from these points into the mafic layer. Arroyo Salado granodiorite along the Arroyo Salado; e) Microgranular dioritic enclaves in the Playas Doradas pluton.**

TABLE I | **AMS data for the Late Paleozoic plutonic rocks in the study area. Kmean: geometric mean of bulk susceptibility for each site. P´: anisotropy degree (Jelinek, 1978), K1 and K3: direction of maximum and minimum susceptibility axes. Location of sites in Figure 4.**

Geologic Unit	Site	Kmean (10^{-5} SI)	P´	*K1* (Az°, Dip°)	*K3* (Az°, Dip°)
Yaminué Complex	V71	1258.6	1.562	356, 21	166, 69
	V79	47.5	1.310	84,12	255, 77
	V80	1033.5	1.233	269, 11	142, 72
	V81	769.6	1.396	297, 9	190, 63
	V82A	20.9	1.110	150, 3	304, 86
	V82B	14.0	1.086	180, 5	43, 84
	V83	6.0	1.040	14, 7	237, 80
	V84	1138.8	1.451	156, 11	10, 77
	V85	787.0	1.295	29, 8	232, 81
	V35	28.3	1.035	356, 11	188, 79
Tardugno Granodiorite	V3	30.2	1.048	75, 24	266, 65
	V10	214.8	1.070	35, 16	154, 60
Cabeza de Vaca Leucogranite	V57	16.1	1.063	98, 9	195,34
	V58	29.2	1.086	119,10	220, 46
	V59	862.3	1.079	8, 47	212, 40
	V61	17.4	1.021	22, 62	247, 20
	V62	23.5	1.012	38, 44	217, 46
	V63	42.9	1.024	86, 23	211, 54
	V69	229.4	1.046	105, 15	248, 71
	V72	29.3	1.053	8, 33	264, 21
	V89	9.2	1.063	5, 3	220, 86

TABLE I | **Continued.**

Geologic Unit	Site	Kmean (10^{-5} SI)	P´	*K1* (Az°, Dip°)	*K3* (Az°, Dip°)
Navarrete Plutonic Complex					
Robaina Facies	V52	48.8	1.014	191, 64	355, 25
	V53	2048.1	1.068	251, 3	343, 28
	V55	1302.6	1.084	261,28	8, 28
	V56	205.8	1.045	313, 17	46, 8
	V64	818.0	1.104	79, 21	284, 67
	V66	704.5	1.071	61, 30	270, 56
	V68	849.1	1.097	241, 12	353, 61
	V86	1478.6	1.049	271, 3	14, 75
	V88	770.2	1.150	71, 14	223, 74
Guanacos Facies	V24	4769.6	1.037	59, 13	315, 46
	V25	3863.0	1.085	108, 3	205, 70
	V28	2253.2	1.111	111, 4	214, 72
	V60	30.3	1.032	170, 18	283, 49
	V65	3686.9	1.115	65, 0	333, 84
	V67	1255.9	1.092	59, 26	226, 63
	V70	1365.6	1.168	67, 33	299, 44
	V87	546.7	1.065	34, 24	282, 41
	V47	3025.0	1.168	237, 53	339, 9
	V48	3372.6	1.125	90, 50	190, 8
	V76	1276.5	1.080	114, 27	224, 33
	V91	604.2	1.056	187, 27	287, 18
Aranda Facies	V2	1544.8	1.108	131, 50	344, 35
	V5	316.9	1.089	300, 40	197, 14
	V8	828.7	1.069	127, 69	35, 1

TABLE I | **Continued.**

Geologic Unit	Site	Kmean (10^{-5} SI)	P´	*K1* (Az°, Dip°)	*K3* (Az°, Dip°)
	V14	1585.0	1.119	231, 12	128, 46
	V15	1007.0	1.075	294, 2	26, 42
	V16	1817.9	1.084	255, 13	151, 44
	V17	1265.1	1.153	130, 2	221, 7
	V18	2028.1	1.220	256, 8	164, 11
	V38	33.4	1.035	338, 50	100, 24
	V51	33.6	1.034	171, 49	75, 5
	V73	937.5	1.121	324, 32	94, 46
	V74	806.1	1.088	324, 33	93, 45
	V77	1836.0	1.295	181, 28	310, 49
	V92	740.7	1.080	213, 26	306, 8
	V93	439.2	1.084	198, 26	294, 13
San Martin Pluton	V44	12.1	1.022	6, 69	115, 7
	V45	24.6	1.028	194, 11	288, 19
	V46	150.8	1.05	19, 10	289, 3

TABLE II | **Mineral Chemistry data. Mineral chemistry was calculated using a JEOL Superprobe JXA-8900-M equipped with five crystal spectrometers at the Luis Brú Electron Microscopy Center, Complutense University, Madrid, Spain. Operating conditions were: acceleration voltage of 15 kV, probe current of 20 nA, with a beam diameter between 1 to 2 µm. Absolute abundances for each element were determined by comparison with standards (Jarosewich et al., 1980; McGuire et al., 1992). An on-line ZAF program was used.**

	SiO_2	Al_2O_3	FeO	MnO	MgO	CaO	Na_2O	K_2O	TiO_2	Cr_2O_3	Total
V80S8	41.40	11.23	17.95	0.36	8.81	11.47	1.11	1.37	0.68	0.04	94.40
V80S9	41.23	11.68	18.05	0.29	8.91	11.61	1.28	1.36	0.58	0.02	95.01
V80S14	42.31	10.37	17.13	0.30	9.62	11.51	1.06	1.18	0.95	-	94.42
V80S31	42.51	9.53	16.95	0.29	10.33	11.40	1.23	1.04	0.90	-	94.17
V80S32	41.53	10.16	17.58	0.43	9.82	11.43	1.14	1.09	0.77	0.10	94.05
V80S33	41.76	10.40	17.84	0.34	9.60	11.67	1.26	1.21	0.99	0.05	95.11
V65S8	45.97	7.75	13.86	0.68	12.13	11.72	1.04	1.00	1.27	0.03	95.44
V65S9	44.22	8.59	16.03	0.77	11.43	11.37	1.23	0.98	1.06	-	95.67
V65S10	45.89	8.11	15.51	0.76	11.93	11.51	1.07	0.75	0.65	0.01	96.20
V65S16	46.07	7.56	15.61	0.73	11.85	11.69	1.02	0.83	1.14	0.03	96.54
V65S17	46.43	7.34	15.15	0.63	12.44	11.57	0.98	0.84	1.14	0.01	96.52
V65S28	46.74	7.54	15.15	0.67	12.28	11.69	1.10	0.84	1.22	0.07	97.30
V65S29	44.65	8.25	15.71	0.74	11.64	11.59	1.26	1.00	1.33	0.01	96.18
V65S30	46.36	7.91	15.32	0.58	12.37	11.80	1.19	0.81	1.24	0.04	97.60
V65S31	45.81	8.39	16.79	0.71	11.71	11.71	1.20	0.90	1.06	0.02	98.30
V65bS162	43.05	8.33	17.04	0.03	10.60	11.47	1.27	1.00	1.42	0.03	94.24
V65bS163	45.14	7.72	16.34		11.70	11.81	1.14	0.85	1.28	0.01	95.99
V65bS165	45.41	7.05	15.31		12.04	11.66	1.38	0.86	1.31	0.00	95.02
V65bS166	44.42	7.55	16.01	0.01	11.24	11.63	1.29	0.81	1.25	0.06	94.27
V91S35	44.95	8.21	17.63	0.02	10.75	10.98	1.54	0.77	0.85	0.04	95.74
V91S41	44.65	8.82	17.03	-	10.46	10.85	1.48	0.96	1.05	0.08	95.37
V91S42	45.67	7.58	17.50	0.02	11.06	10.93	1.58	0.84	0.73	0.02	95.93
V91S43	45.47	8.02	17.07	0.04	10.98	11.29	1.20	0.84	0.73	-	95.65
V91S44	42.20	11.04	18.49	0.04	9.22	10.97	1.76	1.15	1.10	0.02	95.98
V91S52	44.37	9.06	17.59	0.05	10.80	11.16	1.64	0.82	1.04	0.03	96.54
V91S58	43.58	9.26	18.32	0.05	10.12	10.91	1.60	1.00	0.95	0.03	95.81
V91S61	46.23	7.63	17.05	0.03	11.19	10.82	1.41	0.91	0.66	0.04	95.96
V91S62	42.33	10.39	18.29	0.01	9.55	11.09	1.55	1.10	1.17	0.00	95.49
V91S63	44.99	7.09	16.66	0.04	11.35	11.20	1.20	0.67	0.62	0.01	93.84
V91S64	44.49	8.42	17.41	0.05	10.78	11.32	1.39	0.73	1.02	0.10	95.70
V91S69	45.89	7.93	16.62	0.07	11.61	11.20	1.87	0.62	0.96	0.02	96.78

TABLE II | **Continued.**

	SiO_2	Al_2O_3	FeO	MnO	MgO	CaO	Na_2O	K_2O	TiO_2	Cr_2O_3	Total
V91S70	46.05	6.92	16.81	0.03	11.83	11.10	1.22	0.72	0.51	0.00	95.18
V91S71	44.80	8.07	17.45	0.02	11.03	11.19	1.66	0.73	1.05	0.03	96.03
V74S51	47.91	6.71	13.13	0.40	13.72	11.67	1.31	0.73	0.83		96.39
V74S53	48.53	6.12	13.79	0.57	14.33	11.90	1.15	0.57	0.66	0.05	97.68
V74S58	44.99	8.35	14.81	0.58	12.27	11.39	1.38	0.95	1.16		95.87
V74S60	50.91	4.30	11.45	0.63	15.31	11.91	0.89	0.41	0.46	0.01	96.28
V74S61	47.84	5.40	12.82	0.54	14.44	11.50	1.09	0.48	0.56	0.02	94.69
V74S62	45.51	8.13	13.97	0.49	13.09	11.63	1.50	0.81	0.95	0.01	96.08
V74S67	49.99	4.94	12.84	0.66	14.81	11.85	0.93	0.45	0.53	0.02	97.01
V74S68	49.34	5.57	12.86	0.53	14.71	11.52	1.13	0.52	0.71	0.03	96.91
V74S71	46.03	7.78	13.93	0.52	13.21	11.83	1.37	0.75	0.95		96.37
V74S72	50.71	4.79	11.96	0.66	14.65	11.93	0.96	0.40	0.40	0.03	96.50
V74S74	46.93	6.56	13.09	0.62	13.17	11.77	1.22	0.62	0.75		94.73
V74S76	50.97	4.02	10.95	0.63	15.95	11.91	0.83	0.35	0.49	0.05	96.14
V74S77	49.32	4.00	11.74	0.68	14.80	11.74	0.72	0.43	0.47	0.09	93.99
V74S80	47.71	5.96	12.78	0.47	13.92	11.56	1.25	0.64	0.60	0.01	94.91
V74S81	44.68	7.60	13.55	0.63	12.54	11.49	1.36	0.84	1.12	0.05	93.85
V74S82	45.70	8.17	14.06	0.51	12.15	10.39	1.43	0.88	0.97	0.01	94.25
V74S83	49.08	4.99	12.05	0.46	14.79	11.50	1.09	0.47	0.60	0.03	95.06
VAL221S85	45.95	7.96	13.62	-	13.50	11.65	1.27	0.63	1.74	0.05	96.35
VAL221S86	51.83	2.43	13.75	0.05	13.82	12.09	0.34	0.13	0.09	0.04	94.58
VAL221S90	46.48	7.28	13.88	-	13.48	11.74	1.01	0.69	0.93	0.01	95.50
VAL221S107	46.82	6.79	13.93	0.02	13.34	11.51	0.94	0.58	0.35	0.00	94.28
VAL221S108	47.23	6.74	13.17	0.03	13.77	11.64	0.85	0.56	0.29	0.00	94.27
VAL221S109	46.83	6.92	12.91	0.02	13.68	11.56	1.02	0.47	0.42	0.02	93.85
VAL221S131	46.26	7.08	13.75	0.01	13.23	11.10	1.06	0.53	0.99	0.06	94.06
VAL221S134	48.73	4.72	12.38	-	14.84	11.62	0.60	0.37	0.53	0.17	93.97
VAL221S136	48.02	6.65	13.17	-	13.98	11.79	0.72	0.48	0.78	0.04	95.63
VAL221S137	46.57	6.99	13.68	-	13.68	10.61	1.35	0.38	0.94	0.03	94.24

Plagioclase

	SiO_2	Al_2O_3	FeO	CaO	Na_2O	K_2O	Total
V80S1	56.35	26.37	0.11	8.89	6.86	0.28	98.86
V80S2	57.23	25.96	0.09	8.28	7.18	0.25	98.98
V80S3	56.85	25.49	0.10	7.83	7.39	0.25	97.89
V80S16	56.72	26.25	0.09	8.15	6.88	0.30	98.38
V80S18	57.62	26.06	0.11	7.58	7.23	0.23	98.83
V80S19	56.30	26.27	0.02	8.33	6.92	0.16	98.01
V80S20	57.32	26.15	0.11	7.87	7.09	0.33	98.87

TABLE II | **Continued.**

	SiO_2	Al_2O_3	FeO	CaO	Na_2O	K_2O	Total
V80S21	58.24	25.59	0.11	6.94	7.69	0.12	98.69
V80S24	57.69	25.41	0.07	7.33	7.51	0.31	98.32
V80S26	56.74	25.95	0.05	8.00	6.93	0.29	97.95
V80S25	56.33	25.43	0.07	7.27	7.32	0.38	96.80
V80S27	58.37	23.95	0.09	6.70	7.73	0.25	97.10
V80S30	57.02	26.06	0.10	8.04	7.23	0.13	98.57
V65S1	60.54	25.43	0.137	6.08	7.81	0.155	99.87
V65S43	58.28	27.21	0.08	8.02	6.74	0.13	100.47
V65S41	58.24	24.70	0.05	6.95	6.97	0.07	96.98
V65S42	58.26	26.73	0.11	7.59	6.94	0.11	99.73
V65S2	58.91	26.35	0.19	7.37	7.15	0.23	100.21
V65S21	59.32	25.50	0.12	6.54	7.51	0.20	99.18
V65S22	58.94	25.80	0.12	6.80	7.03	0.29	98.98
V65S23	60.86	25.81	0.11	6.27	7.90	0.13	101.08
V65S48	58.38	27.18	0.17	8.03	6.85	0.16	100.76
V65S3	65.55	21.33		1.62	10.23	0.15	98.88
V65S40	60.57	25.77	0.05	6.68	7.54	0.12	100.74
V65bS150	58.22	25.83	0.05	7.74	7.03	0.14	99.00
V65bS151	58.34	25.60	0.07	7.58	7.40	0.10	99.09
V65bS153	57.46	25.80	0.10	8.02	7.03	0.18	98.58
V65bS155	57.28	26.05	0.09	8.19	7.17	0.10	98.88
V65bS156	58.05	25.18	0.08	7.36	7.33	0.15	98.15
V65bS157	56.93	26.15	0.07	8.65	6.75	0.09	98.65
V65bS159	53.96	27.76	0.09	10.61	5.69	0.10	98.21
V65bS161	58.36	25.59	0.14	7.48	7.44	0.06	99.06
V65bS172	57.27	25.58	0.12	7.87	7.06	0.13	98.04
V65bS173	58.00	25.96	0.16	7.64	7.26	0.14	99.16
V91S46	65.34	21.60	0.09	2.60	10.10	0.19	99.93
V91S47	64.41	22.03	0.17	3.22	9.87	0.24	99.94
V91S48	64.34	22.38	0.05	3.23	9.66	0.23	99.89
V91S49	64.45	22.42	0.16	3.26	9.40	0.21	99.92
V91S50	64.83	21.98	0.10	2.89	9.90	0.22	99.93
V91S59	64.91	21.96	0.08	2.97	9.84	0.20	99.96
V91S60	65.10	21.89	0.03	2.74	9.99	0.16	99.90
V91S66	63.95	22.42	0.07	3.41	9.74	0.27	99.86
V91S67	64.73	22.11	0.08	2.89	9.86	0.17	99.82
V91S68	64.29	22.55	0.07	3.36	9.48	0.18	99.93
V91S72	64.96	21.53	0.13	2.60	10.22	0.35	99.80
V91S73	63.96	22.57	0.14	3.46	9.45	0.33	99.90
V91S74	63.94	22.63	0.14	3.61	9.15	0.43	99.90
V91S75	64.06	22.38	0.04	3.23	9.98	0.15	99.84

TABLE II | **Continued.**

	SiO_2	Al_2O_3	FeO	CaO	Na_2O	K_2O	Total
V91S76	63.52	22.77	0.10	3.79	9.60	0.15	99.93
V91S77	63.41	22.70	0.12	3.73	9.49	0.33	99.79
V91S78	60.35	24.52	0.11	6.27	8.25	0.40	99.91
V91S79	59.77	25.36	0.18	6.69	7.60	0.31	99.91
V91S80	58.60	26.03	0.10	7.91	6.99	0.24	99.88
V91S81	60.22	25.05	0.15	6.33	7.87	0.18	99.80
V74S73	68.50	20.17	0.08	0.41	11.01	0.08	100.23
V74S75	64.83	22.72	0.08	2.99	9.64	0.20	100.46
V74S78	63.82	23.30	0.10	3.81	9.14	0.13	100.31
V74S85	58.71	26.39	0.11	7.54	6.81	0.17	99.72
V74S86	55.95	23.31	0.14	9.86	6.56	0.13	95.95
V74S87	58.61	25.86	0.11	6.81	7.25	0.19	98.83
V74S88	64.10	22.90	0.18	3.34	9.37	0.16	100.05
VAL221S92	57.88	24.82	0.11	7.64	6.07	1.21	97.72
VAL221S93	46.58	28.59	0.19	19.69	1.58	0.27	96.89
VAL221S94	43.81	26.44	0.13	22.27	0.53	0.67	93.84
VAL221S100	54.04	27.91	0.28	10.57	5.34	0.11	98.24
VAL221S101	55.25	26.46	0.23	9.51	6.20	0.16	97.80
VAL221S102	53.17	28.72	0.24	11.61	4.93	0.15	98.82
VAL221S110	58.93	24.81	0.14	7.18	7.50	0.19	98.75
VAL221S111	51.23	29.67	0.19	12.64	4.16	0.13	98.01
VAL221S112	59.82	24.35	0.09	6.20	8.09	0.20	98.75
VAL221S113	51.22	30.01	0.19	13.13	4.19	0.12	98.85
VAL221S116	56.34	26.67	0.19	8.82	6.60	0.17	98.79
VAL221S121	57.15	25.67	0.21	8.04	6.66	0.21	97.93
VAL221S123	55.70	27.36	0.21	9.44	6.13	0.13	98.97
VAL221S127	48.93	31.00	0.37	14.20	3.32	0.09	97.91
VAL221S129	56.58	26.81	0.20	9.03	6.37	0.21	99.20
VAL221S130	52.78	28.99	0.16	11.83	4.84	0.13	98.73
VAL221S139	57.64	26.01	0.16	8.16	6.84	0.16	98.96